General constrained conservation laws. Application to pedestrian flow modeling.

Christophe Chalons, Paola Goatin, Nicolas Seguin

General constrained conservation laws. Application to pedestrian flow modeling.

C. Chalons* P. Goatin† N. Seguin‡

July 2, 2012

Abstract

We generalize the results on conservation laws with local flux constraint obtained in [1, 9] to general flux functions and nonclassical solutions arising for example in pedestrian flow modeling. We first define the constrained Riemann solver and the entropy condition, which singles out the unique admissible solution. We provide a well posedness result based on wave-front tracking approximations and Kruzhkov doubling of variable technique. We then provide the framework to deal with nonclassical solutions and we propose a "front-tracking" finite volume scheme allowing to sharply capture classical and nonclassical discontinuities. Numerical simulations illustrating the Braess paradox are presented as validation of the method.

Keywords: Control of conservation laws, Constrained hyperbolic PDE's, Traffic management.

1 Introduction

Several phenomena displayed by vehicular traffic can be modeled using conservation laws in one space-dimension, see for example [18] for a survey of available models. In particular, specific situations as the presence of toll gates, construction sites, or even moving bottlenecks caused by slow moving large vehicles, can be realistically modeled by imposing a local constraint on the flux, see [9, 10, 11, 16, 17]. In all these works, the flux function of the involved model is assumed to be concave, which strongly simplifies the structure and the analysis of solutions.

*Université Paris Diderot-Paris 7 & Laboratoire J.-L. Lions, U.M.R. 7598, UMPC, Boîte courrier 187, 75252 Paris Cedex 05, France. E-mail: christophe_chalons@ljll.univ-paris-diderot.fr

†INRIA Sophia Antipolis - Méditerranée, EPI OPALE, 2004, route des Lucioles - BP 93, 06902 Sophia Antipolis Cedex, France. E-mail: paola.goatin@inria.fr

‡UPMC Univ Paris 06 & CNRS UMR 7598, Laboratoire J.-L. Lions, 75005 Paris, France. E-mail: nicolas.seguin@upmc.fr

Besides, Colombo and Rosini [12] introduced a model for pedestrian flow accounting for panic appearance and consisting in a scalar conservation law in one space-dimension displaying nonclassical shocks. Such a simplified model can be used for example to describe the motion of a crowd along a corridor or a bridge. Moreover, in [13] the authors show that the flux constraint represented by the presence of a door may cause the onset of panic states from a normal situation. In this model, the flux function is not concave (nor convex) and therefore it does not match the available results about conservation laws with constrained flux. A rigorous analysis of this pedestrian flow model thus needs the extension of the above cited results to general fluxes.

The aim of this paper is to study the Cauchy problem for scalar conservation laws with local unilateral constraint of the form

$$\partial_t \rho + \partial_x f(\rho) = 0, \qquad t > 0,\ x \in \mathbb{R}, \tag{1.1}$$

$$\rho(0,x) = \rho_0(x), \qquad x \in \mathbb{R}, \tag{1.2}$$

$$f(\rho(t,0)) \leq F(t), \qquad t > 0. \tag{1.3}$$

In connection with problem (1.1)-(1.3), we fix $R > 0$ to be the maximal density supported by the model and we assume that the flux function $f : [0,R] \to \mathbb{R}$ is Lipschitz continuous with Lipschitz constant L

(F.1) $f \in \mathbf{W}^{1,\infty}\big([0,R];[0,+\infty[\big)$,

and satisfies

(F.2) $f(\rho) \geq 0,\ \ f(0) = f(R) = 0$,

(F.3) there exists a finite set of points $\{\rho_1, \ldots, \rho_N\} \subset [0,R]$, $N \geq 1$, s.t. $f'(\rho)(\rho_i - \rho) \neq 0 \qquad i = 1, \ldots, N$, a.e. in $[0,R]$.

We will also denote by $f_{\max}$ the maximum of f on $[0,R]$:

$$f_{\max} = \max_{\rho \in [0,R]} f(\rho).$$

The paper is organized as follows. In Section 2 we define the constrained Riemann solver and the entropy condition associated to (1.1)-(1.3). This allows to prove a well posedness result based on wave-front tracking approximations and Kruzhkov doubling of variable technique. (Details of the proof are collected in Section 6.) Section 3 revises the finite volume scheme introduced in [1]. Finally, Sections 4 and 5 deal with nonclassical solutions to the pedestrian flow model proposed in [12]: we define the constrained nonclassical Riemann solver and we propose a "front-tracking" finite volume scheme allowing to sharply capture classical and nonclassical discontinuities. Numerical simulations illustrating the Braess paradox are presented in Section 5.3.

2 Well posedness

2.1 Definition of the constrained Riemann solver

Let $\mathcal{R}$ be the standard Liu [21] Riemann solver for (1.1), (1.2), with

$$\rho(0,x) = \begin{cases} \rho_l \text{ if } x < 0, \\ \rho_r \text{ if } x > 0, \end{cases} \tag{2.1}$$

so that the map $(t,x) \mapsto \mathcal{R}(\rho_l,\rho_r)(x/t)$ is the standard weak entropy solution to (1.1),(2.1).

Let $F(t) \equiv F \in [0, f_{\max}]$ be constant, and $\rho_1^F, \dots, \rho_M^F \in [0,R]$, $2 \le M \le N+1$, be the roots of the equation

$$f(\rho) = F.$$

In connection with (2.1), we denote

$$\hat\rho_l^F = \begin{cases} \min\left\{\rho_1^F,\dots,\rho_M^F \colon \rho_i^F \ge \rho_l\right\} & \text{if } f(\rho_l) > F \\ \max\left\{\rho_1^F,\dots,\rho_M^F \colon \rho_i^F \le \rho_l\right\} & \text{if } f(\rho_l) \le F \end{cases} \tag{2.2}$$

$$\check\rho_r^F = \begin{cases} \max\left\{\rho_1^F,\dots,\rho_M^F \colon \rho_i^F \le \rho_r\right\} & \text{if } f(\rho_r) > F \\ \min\left\{\rho_1^F,\dots,\rho_M^F \colon \rho_i^F \ge \rho_r\right\} & \text{if } f(\rho_r) \le F \end{cases} \tag{2.3}$$

whenever $\rho_l > \rho_1^F$, respectively $\rho_r < \rho_M^F$.

Remark 1 In particular, we observe that

$$f'(\hat\rho_l^F) \le 0, \qquad f'(\check\rho_r^F) \ge 0 \tag{2.4}$$

(if the derivative is defined). Therefore, a stationary jump from $\hat\rho_l^F$ to $\check\rho_r^F$ doesn't satisfy the Lax entropy condition (and a fortiori Liu's entropy condition). We will refer to such discontinuities as *nonclassical shocks*.

Definition 2.1 *The constrained Riemann solver* $\mathcal{R}^F : (\rho_l,\rho_r) \mapsto \mathcal{R}^F(\rho_l,\rho_r)$ *for* (1.1)-(1.3) *is defined as follows.*
If $f\left(\mathcal{R}(\rho_l,\rho_r)(0)\right) \le F$, *then* $\mathcal{R}^F(\rho_l,\rho_r) = \mathcal{R}(\rho_l,\rho_r)$.
Otherwise, $\mathcal{R}^F(\rho_l,\rho_r)(\lambda) = \begin{cases} \mathcal{R}(\rho_l,\hat\rho_l^F)(\lambda) \ \textit{if } \lambda < 0\,, \\ \mathcal{R}(\check\rho_r^F,\rho^r)(\lambda) \ \textit{if } \lambda > 0\,. \end{cases}$

We now check that Definition 2.1 defines a self-similar weak solution to (1.1), (2.1), subject to the constant constraint F. First of all, we remind that the classical entropy Riemann solver satisfies

$$f\left(\mathcal{R}(\rho_l,\rho_r))(0)\right) = \begin{cases} \min\limits_{\rho\in[\rho_l,\rho_r]} f(\rho) & \text{if } \rho_l \le \rho_r\,, \\ \max\limits_{\rho\in[\rho_r,\rho_l]} f(\rho) & \text{if } \rho_r < \rho_l\,. \end{cases} \tag{2.5}$$

Let us analyze the left-hand side of the solution (i.e. for $\lambda < 0$, the analysis for $\lambda > 0$ being similar). First of all, let us observe that if $f\big(\mathcal{R}(\rho_l, \rho_r)(0)\big) > F$, then (2.5) implies $\rho_l > \rho_1^F$. We have to distinguish several cases.

- If $\rho_l \le \rho_1^F$, we have by (2.5)

$$f\big(\mathcal{R}(\rho_l, \rho_r)(0)\big) \le F, \text{ hence } \mathcal{R}^F(\rho_l, \rho_r) = \mathcal{R}(\rho_l, \rho_r).$$

- If $f(\rho_l) > F$, then by (2.2) $\hat\rho_l^F > \rho_l$ and (2.5) implies

$$f(\mathcal{R}(\rho_l, \hat\rho_l^F)(0)) = \min_{\rho \in [\rho_l, \hat\rho_l^F]} f(\rho) = f(\hat\rho_l^F) = F,$$

  hence $\mathcal{R}(\rho_l, \hat\rho_l^F)$ does not contain waves with positive speed.

- If $f(\rho_l) \le F$ and $\rho_l > \rho_1^F$, then by (2.2) $\hat\rho_l^F \le \rho_l$ and (2.5) implies

$$f(\mathcal{R}(\rho_l, \hat\rho_l^F)(0)) = \max_{\rho \in [\hat\rho_l^F, \rho_l]} f(\rho) = f(\hat\rho_l^F) = F,$$

  hence again $\mathcal{R}(\rho_l, \hat\rho_l^F)$ does not contain waves with positive speed.

It can be easily checked that, in Definition 2.1, the traces of the discontinuity at $x = 0$ satisfy

$$\check\rho_r^F \le \hat\rho_l^F$$

and the resulting shock is non-entropic by (2.4), see Remark 1.

2.2 Entropy conditions

Having in mind the analysis of the model for pedestrian flow introduced in [12], and in order to reduce technicalities and the number of cases to be considered, from now on we will restrict the study to flux functions that fit the hypotheses in [13]. Nevertheless, we believe that the results hold true for more general fluxes. We will require the following properties (see Fig. 1, right, in Section 4):

(F.2) $f(\rho) = 0$ if and only if $\rho \in \{0, R\}$;
(F.3) f has a local minimum at $r \in [0, R]$
(F.4) the restrictions $f_{|[0,r]}$ and $f_{|[r,R]}$ are strictly concave;
(F.5) $f(R_M) = \max\big\{f(\rho)\colon \rho \in]0, r[\big\} > f(R_M^*) = \max\big\{f(\rho)\colon \rho \in]r, R[\big\}$.

Further requirements will be added in Section 4.

The definitions of entropy weak solutions introduced in [1, 9] can be generalized to the present case. Let us introduce the function

$$\Phi(a, b) = \operatorname{sgn}(a - b)\big(f(a) - f(b)\big) = f(a \top b) - f(a \bot b),$$

where $a \top b = \max\{a, b\}$ and $a \bot b = \min\{a, b\}$.

Definition 2.2 *A function $\rho \in \mathbf{L}^\infty(\mathbb{R}^+ \times \mathbb{R}; [0,R])$ is a weak entropy solution of (1.1)-(1.3) if*
(i) it satisfies the following entropy inequalities: for every $\varphi \in \mathbf{C^1_c}(\mathbb{R}^+ \times \mathbb{R}; \mathbb{R}^+)$ and all $\kappa \in [0,R]$,

$$\int_0^{+\infty} \int_{\mathbb{R}} (|\rho(t,x) - \kappa| \partial_t + \Phi(\rho(t,x),\kappa)\partial_x)\ \varphi(t,x)\ dx\ dt$$
$$+ \int_{\mathbb{R}} |\rho_0(x) - \kappa|\ \varphi(0,x)\ dx + 2\int_0^{+\infty} \big(f(\kappa) - f(\kappa) \perp F(t)\big)\, \varphi(t,0)\ dt \geq 0, \tag{2.6}$$

(ii) it verifies the constraint:

$$f(\rho(t,0-)) = f(\rho(t,0+)) \leq F(t) \quad \text{for a.e. } t > 0, \tag{2.7}$$

where $\rho(t,0\pm)$ denote the operators of left and right strong traces at $\{x = 0\}$.

Remark 2 Condition (2.6) differs from the entropy condition given in [9] in the last integrand. More precisely, the condition given here is finer, in the sense that (2.6) implies the inequality [9, (3.2)]. In fact it is straightforward to check that

$$f(\kappa) - f(\kappa) \perp F(t) \leq \left(1 - \frac{F(t)}{f_{\max}}\right) f(\kappa), \quad \text{for all } t > 0,\ \kappa \in [0,R].$$

Moreover, condition [9, (3.2)] does not work in the setting of non-concave fluxes, since it is not sufficient to rule out some non-admissible nonclassical stationary shocks.

Condition (2.6) was first found by the authors when passing to the limit in the discrete entropy inequality for finite volume approximations (see the proof of [1, Proposition 4.7]).

It is easy to check that the constrained Riemann solver introduced in Definition 2.1 gives a weak entropy solution of (1.1)-(1.3) in the sense of the above Definition 2.2.

Proposition 2.3 *Let $\rho(t,x) = \mathcal{R}^F(\rho_l, \rho_r)(x/t)$ be the solution to (1.1), (1.3) and (2.1) constructed in Definition 2.1. Then ρ is a weak entropy solution in the sense of Definition 2.2. Moreover, the entropy condition (2.6) and the constraint (2.7) single out the admissible stationary discontinuities at $x = 0$.*

Proof. Let us consider an admissible nonclassical stationary shock at $x = 0$, i.e. assume $\rho(t,0-) = \hat{\rho}_l^F$ and $\rho(t,0+) = \check{\rho}_r^F$. In particular, we know that $f(\hat{\rho}_l^F) = f(\check{\rho}_r^F) = F$ and $\hat{\rho}_l^F > \check{\rho}_r^F$. Consider now a nonnegative test function

$\xi \in \mathbf{C_c^1}((0,+\infty))$ and take $\varphi_\varepsilon = w_\varepsilon \xi$ with $\varepsilon > 0$ in (2.6). Here w_ε is the cut-off function defined by

$$w_\varepsilon(x) = \begin{cases} 1 & \text{if } |x| < \varepsilon, \\ 2 - |x|/\varepsilon & \text{if } \varepsilon \le |x| \le 2\varepsilon, \\ 0 & \text{if } |x| > 2\varepsilon. \end{cases} \tag{2.8}$$

Then the entropy inequality (2.6) becomes

$$I(\varepsilon) + J(\varepsilon) \ge 0,$$
$$I(\varepsilon) = \int_0^{+\infty} \int_{\mathbb{R}} (|\rho - \kappa| \partial_t \xi + \Phi(\rho, \kappa) \partial_x \xi)\ w_\varepsilon\ dx\ dt,$$
$$J(\varepsilon) = \int_0^{+\infty} \int_{\mathbb{R}} \Phi(\rho, \kappa) \xi w_\varepsilon'\ dx\ dtx + 2 \int_0^{+\infty} \big(f(\kappa) - f(\kappa) \perp F(t)\big)\ \xi(t)\ dt.$$

Clearly, $\lim_{\varepsilon \to 0} I(\varepsilon) = 0$. Moreover, using the definition of traces, we deduce

$$\lim_{\varepsilon \to 0} J(\varepsilon) = \int_0^{+\infty} \Big(\Phi(\rho(t,0-), \kappa) - \Phi(\rho(t,0+), \kappa) + 2 \big(f(\kappa) - f(\kappa) \perp F(t)\big) \Big) \xi(t)\ dt,$$

which gives for all $\kappa \in [0,1]$ and a.e. $t > 0$

$$\Phi(\rho(t,0-), \kappa) - \Phi(\rho(t,0+), \kappa) + 2 \big(f(\kappa) - f(\kappa) \perp F(t)\big) \ge 0. \tag{2.9}$$

In our case, (2.9) writes

$$\Phi(\hat{\rho}_l^F, \kappa) - \Phi(\check{\rho}_r^F, \kappa) + 2 \big(f(\kappa) - f(\kappa) \perp F(t)\big) \ge 0. \tag{2.10}$$

To check (2.10), let us consider the case $\check{\rho}_r^F \le \kappa \le \hat{\rho}_l^F$, so that the left hand side of (2.10) rewrites

$$\begin{aligned} & f(\hat{\rho}_l^F) - f(\kappa) - f(\kappa) + f(\check{\rho}_r^F) + 2 \big(f(\kappa) - f(\kappa) \perp F(t)\big) \\ &= 2F - 2f(\kappa) + 2 \big(f(\kappa) - f(\kappa) \perp F(t)\big) \\ &= 2F - 2f(\kappa) \perp F(t) \ge 0. \end{aligned}$$

The cases $\kappa < \check{\rho}_r^F$ and $\kappa > \hat{\rho}_l^F$ can be checked in the same way.

Let us now check that other nonclassical stationary discontinuities are ruled out by (2.6). Assume first that $\rho(t,0-) > \rho(t,0+)$ and $f(\rho(t,0-)) = f(\rho(t,0+)) = \tilde{f} < F$. In this case, (2.9) becomes, for $\rho(t,0+) \le \kappa \le \rho(t,0-)$,

$$\begin{aligned} & f(\rho(t,0-)) - f(\kappa) - f(\kappa) + f(\rho(t,0+)) + 2 \big(f(\kappa) - f(\kappa) \perp F\big) \\ &= 2\tilde{f} - 2f(\kappa) + 2 \big(f(\kappa) - f(\kappa) \perp F\big) \\ &= 2\tilde{f} - 2f(\kappa) \perp F. \end{aligned}$$

If we now choose $\bar{\kappa}$ such that $f(\bar{\kappa}) \geq F$, we get

$$2\tilde{f} - 2f(\bar{\kappa})\perp F(t) = 2\left(\tilde{f} - F\right) < 0,$$

hence the discontinuity is not admissible.

Finally, we consider the case where $\rho(t,0-) < \rho(t,0+)$, with $f(\rho(t,0-)) = f(\rho(t,0+)) = \tilde{f} \leq F$ and there exists $\tilde{\rho} \in]\rho(t,0-), \rho(t,0+)[$ such that $f(\tilde{\rho}) < \tilde{f}$. In this case, for $\rho(t,0-) \leq \kappa \leq \rho(t,0+)$, (2.9) becomes

$$\begin{aligned}
&f(\kappa) - f(\rho(t,0-)) - f(\rho(t,0+)) + f(\kappa) + 2\left(f(\kappa) - f(\kappa)\perp F\right) \\
&= 2f(\kappa) - 2\tilde{f} + 2\left(f(\kappa) - f(\kappa)\perp F\right) \\
&= 4f(\kappa) - 2\tilde{f} - 2f(\kappa)\perp F.
\end{aligned}$$

Taking $\kappa = \tilde{\rho}$ in the above expression we get

$$4f(\tilde{\rho}) - 2\tilde{f} - 2f(\tilde{\rho})\perp F = 2\left(f(\tilde{\rho}) - \tilde{f}\right) < 0.$$

□

In order to formulate a second (equivalent) definition that does not need the explicit condition (2.7) on traces as in [1], we introduce the following sets:

- $\mathcal{G}_1(F) = \{(c_l, c_r) \in [0,R]^2; c_l > c_r, f(c_l) = f(c_r) = F, f(r) > F, \exists r \in [c_r, c_l]\}$,
- $\mathcal{G}_2(F) = \{(c,c) \in [0,R]^2; f(c) \leq F\}$,
- $\mathcal{G}_3(F) = \{(c_l, c_r) \in [0,R]^2; f(c_l) = f(c_r) \leq F,\ (c^* - c_l)(f(c^*) - f(c_l)) \geq 0\ \forall c^* \in [c_l \perp c_r, c_l \top c_r]\}$,

and denote

$$\mathcal{G}(F) = \mathcal{G}_1(F) \cup \mathcal{G}_2(F) \cup \mathcal{G}_3(F).$$

Remark that the sets $\mathcal{G}_2$ and $\mathcal{G}_3$ contain the traces of classical entropy weak solutions (continuous parts or entropy admissible shocks), while $\mathcal{G}_1$ contains the traces of nonclassical discontinuities that can even result by superposition of classical and nonclassical shocks at zero speed. We also define the functions $c : \mathbb{R} \to [0,R]^2$ by

$$c(x) = \begin{cases} c_l & \text{if } x < 0, \\ c_r & \text{if } x > 0, \end{cases} \tag{2.11}$$

with $(c_l, c_r) \in [0,R]^2$.

Definition 2.4 *A function $\rho \in \mathbf{L}^\infty(\mathbb{R}^+ \times \mathbb{R}; [0, R])$ is a weak entropy solution of (1.1)-(1.3) if there exists $M > 0$ such that for every $\varphi \in \mathbf{C_c^1}(\mathbb{R}^+ \times \mathbb{R}; \mathcal{R}^+)$ and all c defined by (2.11),*

$$\int_0^{+\infty} \int_{\mathbb{R}} (|\rho(t,x) - c(x)|\partial_t + \Phi(\rho(t,x), c(x))\partial_x)\ \varphi(t,x)\ dx\ dt$$
$$+ \int_{\mathbb{R}} |\rho_0(x) - c(x)|\ \varphi(0,x)\ dx + M \int_0^{+\infty} \mathrm{dist}\,((c_l, c_r), \mathcal{G}(F(t)))\ \varphi(t,0)\ dt \geq 0. \tag{2.12}$$

Definitions 2.2 and 2.4 are equivalent. In fact we can prove the following

Proposition 2.5 *A function $\rho \in \mathbf{L}^\infty(\mathbb{R}^+ \times \mathbb{R}; [0, R])$ satisfies (2.6)-(2.7) if and only if it satisfies (2.12).*

The proof is detailed in [1, Proof of Proposition 2.6]. We only need to verify that [1, Lemma 2.7] still holds. We report it below for completeness, the proof being postponed to Section 6.

Lemma 2.6 [1, Lemma 2.7]
(i) If $(b_l, b_r) \in \mathcal{G}(F)$, then

$$\forall (c_l, c_r) \in \mathcal{G}(F), \quad \Phi(b_l, c_l) \geq \Phi(b_r, c_r). \tag{2.13}$$

(ii) The converse is true, under the following form:

$$\begin{array}{l} \text{if (2.13) holds and the Rankine-Hugoniot condition} \\ f(b_l) = f(b_r) \text{ is satisfied, then } (b_l, b_r) \in \mathcal{G}(F). \end{array} \tag{2.14}$$

To conclude this section, a well-posedness result for (1.1)-(1.3) can be recovered as in [1] (the proof can be found in Section 6). Nevertheless, in the present (non-concave) case the map $F \mapsto \mathrm{dist}\,((c_l, c_r), \mathcal{G}(F))$ is not continuous as a map in $\mathbf{L^1}_{loc}(\mathbb{R}^+)$ with values in $\mathbb{R}^+$. Therefore, we cannot pass to the limit in the last integral of(2.12). This prevents us from obtaining a well posedness result for $F \in \mathbf{L}^\infty(\mathbb{R}^+; [0, f_{\max}])$.

Theorem 2.7 *For any $\rho_0 \in \mathbf{L}^\infty(\mathbb{R}; [0, R])$ such that $\psi(\rho_0) \in \mathbf{BV}(\mathbb{R}; [0, R])$ and $F \in \mathbf{BV}(\mathbb{R}^+; [0, f_{\max}])$, there exists one and only one entropy solution ρ to Problem (1.1)-(1.3) (in the sense of Definitions 2.2 and 2.4), such that $\psi(\rho(t, \cdot)) \in \mathbf{BV}(\mathbb{R}; [0, R])$ for all $t > 0$. Moreover, assume $F^1, F^2 \in \mathbf{BV}(\mathbb{R}^+; [0, f_{\max}])$, and $\rho_0^1, \rho_0^2 \in \mathbf{L}^\infty(\mathbb{R}, [0, R])$ such that $(\rho_0^1 - \rho_0^2) \in \mathbf{L^1}(\mathbb{R})$ and $\psi(\rho_0^1), \psi(\rho_0^2) \in \mathbf{BV}(\mathbb{R}; [0, R])$. Assume that ρ^1, ρ^2 are entropy solutions of (1.1)-(1.3), corresponding to the initial data ρ_0^1, ρ_0^2 and to the constraints F^1, F^2, respectively. Then, for a.e. $T > 0$, we have*

$$\int_{\mathbb{R}} |\rho^1 - \rho^2|(T, x)\ dx\ \leq\ 2 \int_0^T |F^1 - F^2|(t)\, dt\ +\ \int_{\mathbb{R}} |\rho_0^1 - \rho_0^2|(x)\, dx. \tag{2.15}$$

3 Finite volume numerical schemes for the constrained problem

We now present a class of numerical schemes which easily account for the constraint (1.3). The idea is exactly the same as the one proposed in [1]. First of all, let us present some usual notations. We introduce a space step Δx and a time step Δt, both assumed to be constant, and we set $\nu = \Delta t/\Delta x$. We define the mesh interfaces $x_{j+1/2} = j\Delta x$ for $j \in \mathbb{Z}$ and the intermediate times $t^n = n\Delta t$ for $n \in \mathbb{N}$. At each time t^n, ρ_j^n represents an approximation of the mean value of the solution to (1.1)-(1.2) on the interval $[x_{j-1/2}, x_{j+1/2})$, $j \in \mathbb{Z}$. Therefore, a piecewise constant approximate solution $x \to \rho_\nu(x, t^n)$ is given by

$$\rho_\nu(x, t^n) = \rho_j^n \text{ for all } x \in C_j = [x_{j-1/2}; x_{j+1/2}), \ j \in \mathbb{Z}, \ n \in \mathbb{N}.$$

When $n = 0$, we set

$$\rho_j^0 = \frac{1}{\Delta x} \int_{x_{j-1/2}}^{x_{j+1/2}} \rho_0(x)dx, \text{ for all } j \in \mathbb{Z}.$$

In the case of classical conservation laws (1.1), a well-known class of finite volume approximation is defined by the so-called three-point monotone schemes:

$$\rho_j^{n+1} = \rho_j^n - \frac{\Delta t}{\Delta x}(f_{j+1/2}^n - f_{j-1/2}^n) \tag{3.1}$$

where $f_{j+1/2}^n = g(\rho_j^n, \rho_{j+1}^n)$ for any $j \in \mathbb{Z}$ and $n \in \mathbb{N}$, and g satisfies the following assumptions:

- Smoothness: $g \in \mathcal{C}^1([0, R]^2)$ with Lipschitz constant L_g.
- Consistency: $\forall a \in [0, R]$, $g(a, a) = f(a)$.
- Monotonicity: g is nondecreasing w.r.t. its first variable and nonincreasing w.r.t. its second variable.

Under the CFL condition

$$\nu \leq \frac{1}{2L_g}, \tag{3.2}$$

such a numerical scheme converges to the entropy weak solution of (1.1), (1.2). In [1], the authors proposed to modify such a scheme at the interface where the constraint (1.3) acts:

$$f_{1/2}^n = \min(g(\rho_0^n, \rho_1^n), F(t^n)), \tag{3.3}$$

keeping elsewhere

$$f_{j+1/2}^n = g(\rho_j^n, \rho_{j+1}^n) \quad \forall j \neq 0. \tag{3.4}$$

They proved the convergence of the numerical scheme to the entropy solution of (1.1)-(1.3) in the case of a bell-shaped flux function f. In this section we investigate the extension of such analysis (possibly using different arguments) to flux functions which comply with properties **(F.1)-(F.5)**.

The most important remark is that the local modification of the numerical flux (3.3) do not affect the monotonicity of the scheme:

$$\begin{array}{l}\text{Under condition (3.2),}\\ \rho_j^{n+1} \text{ is a nondecreasing function of } \rho_{j-1}^n,\ \rho_j^n \text{ and } \rho_{j+1}^n.\end{array} \tag{3.5}$$

Therefore, one can easily deduce the $\mathbf{L}^\infty$ bound for the numerical scheme:

$$0 \le \rho_\nu \le R \quad \text{a.e.} \tag{3.6}$$

and, as a result of the Crandall-Tartar lemma [14], we have the discrete time continuity estimate (see [4]):

$$\sum_{j\in\mathbb{Z}} |\rho_j^{n+1} - \rho_j^n| \le |\rho_0|_{\mathbf{BV}(\mathbb{R})}. \tag{3.7}$$

It is clear that it is very difficult to control the variation of the ρ_ν in the space direction due to the nontrivial treatment of the interface. However, one may follow the successful strategy developed in [4]. Using the estimate (3.7), the authors are able to prove $\mathbf{BV}$ bounds far from the interface, let us say on $[-B,-A]\cup[A,B]$, with $0<A<B$. It takes the form for almost any $T>0$

$$|\rho_\nu(T,.)|_{\mathbf{BV}(A,B)} \le |\rho_0|_{\mathbf{BV}(A,B)} + \frac{K}{r} \tag{3.8}$$

where $0<r<A$ and for Δx sufficiently small (smaller than r). Though this bound blows up when $A\to 0$ (since $r\to 0$), convergence as $\Delta x\to 0$ can be achieved on $[-B,-A]\cup[A,B]$ for any fixed A by the Helly's theorem. Therefore, taking a decreasing sequence $(A_m)_m$ and letting Δx tend to 0 for each A_m, one may use the Cantor diagonal process to extract a subsequence to the numerical approximation which converges almost everywhere to a function of $\mathbf{L}^\infty(\mathbb{R}^+\times\mathbb{R})$.

We now have to identify this limit. To do so, we derive the discrete entropy inequalities verified by the numerical scheme. Following [1], one may check that, for any $(k_j)_{j\in\mathbb{Z}}\subset[0,R]$, $j\in\mathbb{Z}$ and $n\in\mathbb{N}$,

$$|\rho_j^{n+1}-\kappa_j| - |\rho_j^n-\kappa_j| + \nu(F_{j+1/2}^n - F_{j-1/2}^n) - \nu H_i^n \le 0 \tag{3.9}$$

where

$$F_{j+1/2}^n = \begin{cases} g(\rho_j^n \top \kappa_i, \rho_{j+1}^n \top \kappa_{j+1}) - g(\rho_j^n \perp \kappa_i, \rho_{j+1}^n \perp \kappa_{j+1}) & \text{if } j\neq 0\\ \min(g(\rho_j^n \top \kappa_i, \rho_{j+1}^n \top \kappa_{j+1}), F(t^n)) & \\ \qquad - \min(g(\rho_j^n \perp \kappa_i, \rho_{j+1}^n \perp \kappa_{j+1}), F(t^n)) & \text{if } j=0 \end{cases}$$

and

$$H_i^n = \begin{cases} |\min(g(\kappa_0,\kappa_1),F(t^n)) - g(\kappa_{-1},\kappa_0)| & \text{if } j=0, \\ |g(\kappa_1,\kappa_2) - \min(g(\kappa_0,\kappa_1),F(t^n))| & \text{if } j=1, \\ 0 & \text{else.} \end{cases}$$

Starting form inequalities (3.9), one may use the proof of the Lax-Wendroff theorem to deduce that any limit $\bar{\rho} \in \mathbf{L}^\infty(\mathbb{R}^+ \times \mathbb{R})$ of the numerical scheme satisfies for all $(c_l, c_r) \in [0,R]^2$

$$\begin{aligned} \int_{\mathbb{R}^+}\int_{\mathbb{R}} (|\bar{\rho}(t,x)-c(x)|\partial_t + \Phi(\bar{\rho}(t,x),c(x))\partial_x)\ \varphi(t,x)\ dx\ dt \\ + \int_{\mathbb{R}} |\rho_0(x)-c(x)|\ \varphi(0,x)\ dx \\ + 12L_g \int_{\mathbb{R}^+} \operatorname{dist}\left((c_l,c_r), \mathcal{G}_1(F(t)) \cup \mathcal{G}_2(F(t))\right)\ \varphi(t,0)\ dt \geq 0 \quad (3.10) \end{aligned}$$

where c is defined by (2.11). The proof can be found in [1], but let us comment the last term. Actually, it attests to the fact that the scheme is able to preserve exactly any initial data $\rho_0(x) = c(x)$ with c given by (2.11) and $(c_l, c_r) \in \mathcal{G}_1(F) \cup \mathcal{G}_2(F)$, as soon as F is constant in t. For the case $(c_l, c_r) \in \mathcal{G}_3(F)$, which corresponds to a stationary shock wave, most of numerical schemes cannot preserve such initial data since they introduce numerical diffusion. The last step is now to prove that if $\bar{\rho}$ satisfies (3.10), then it also satisfies (2.12). Once again, the answer can be found in [1], Lemma 4.8.

4 A nonclassical Riemann solver

The model of pedestrian traffic flow introduced in [12, 13] is based on a flux function f like the one represented in Figure 1. In particular, f has a local minimum at R, which is the maximal density in normal (non-panic) situations, while bigger densities $R < \rho \leq R^*$ can be reached in case of panic.

For simplicity, it is assumed that the restrictions $f_{|[0,R]}$ and $f_{|[R,R^*]}$ are strictly concave. Hence there exists a unique point $R_M \in]0,R[$ such that $f(R_M) = \max\{f(\rho)\colon \rho \in [0,R]\}$ and a unique point $R_M^* \in]R,R^*[$ such that $f(R_M^*) = \max\{f(\rho)\colon \rho \in [R,R^*]\}$.

The evolution of the solutions to (1.1) is governed through the introduction of nonclassical shocks, that violate the maximum principle and then allow the appearance of panic from non-panic regimes.

As it is usual when dealing with nonclassical scalar conservation laws, see [20, Chapter II], in [12] authors introduced the auxiliary functions ψ and φ, see Figure 2, left. Let $\psi(R) = R$ and, for $\rho \neq R$, let $\psi(\rho)$ be such that the straight line through $\big(\rho, f(\rho)\big)$ and $\big(\psi(\rho), f\circ\psi(\rho)\big)$ is tangent to

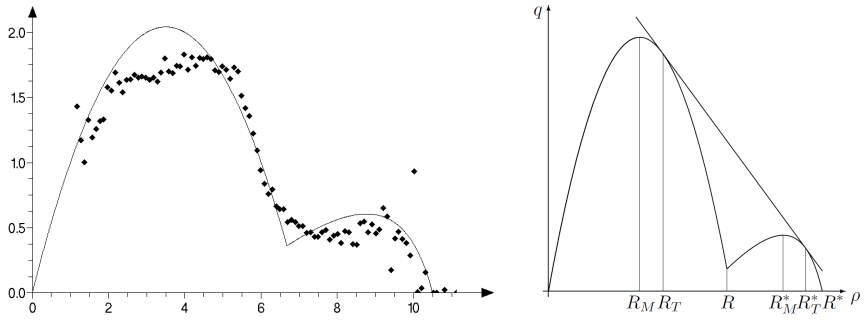

Figure 1: Left, a flow satisfying hypotheses in [13]. Superimposed are experimental measurements from [19]. Crowd density, ρ, is on the horizontal axis and flow, $\rho\, v$, on the vertical one. Right, notations used in the paper. (Figures taken from [10, 13].)

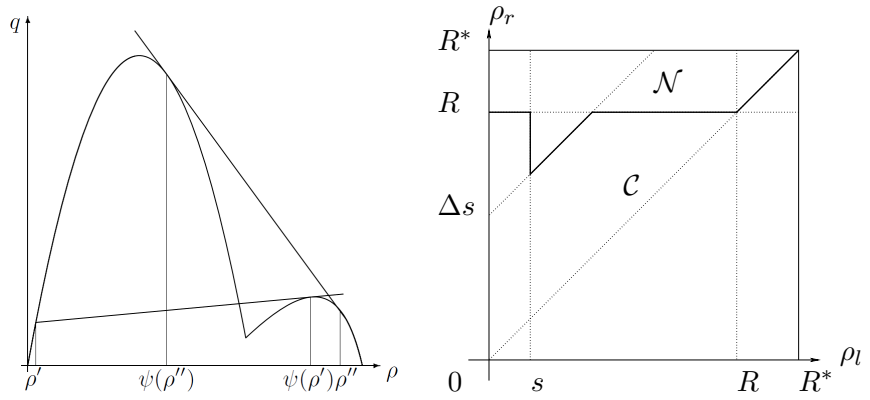

Figure 2: Left, the functions ψ and φ: their geometrical meaning. Right, the Riemann Solver: in $\mathcal{C}$, the solution consists of classical waves only; in $\mathcal{N}$, also nonclassical shocks are present.

the graph of f at $\big(\psi(\rho), f\circ\psi(\rho)\big)$. Let $R_T \in]0, R[$ and $R_T^* \in]R, R^*[$ be such that $\psi(R_T) = R_T^*$ and $\psi(R_T^*) = R_T$ (see Fig. 1, right). Besides, for $\rho \in [0, R_T[$, the line through $\big(\rho, f(\rho)\big)$ and $\big(\psi(\rho), f\circ\psi(\rho)\big)$ has a further intersection with the graph of f, which we call $\big(\varphi(\rho), f\circ\varphi(\rho)\big)$. In [12], the authors introduce two thresholds s and Δs such that

$$s > 0\,,\ \Delta s > 0\,,\ s < R_M \text{ and } R > s + \Delta s \geq \varphi(s) > R_T > R - \Delta s\,. \quad (4.1)$$

Here we will also assume that

$$f(s) > f(R).$$

The nonclassical Riemann solver $\mathcal{R}_{NC}$ is then defined as follows. Let $\mathcal{NS}(\rho_l, \rho_r)$ denote the (nonclassical) shock joining ρ_l to ρ_r and moving with the speed

given by the Rankine-Hugoniot equation

$$\lambda(\rho_l, \rho_r) = \frac{f(\rho_l) - f(\rho_r)}{\rho_l - \rho_r}.$$

- If $\rho_l, \rho_r \in [0, R]$ and $\rho_l > s,\ \rho_r - \rho_l > \Delta s$, then

$$\mathcal{R}_{NC}(\rho_l, \rho_r) = \mathcal{NS}(\rho_l, \psi(\rho_l)) + \mathcal{R}(\psi(\rho_l), \rho_r).$$

- If $\rho_l < R < \rho_r$ and the segment between $(\rho_l, f(\rho_l))$ and $(\rho_r, f(\rho_r))$ intersects the curve $f = f(\rho)$, then

$$\mathcal{R}_{NC}(\rho_l, \rho_r) = \begin{cases} \mathcal{NS}(\rho_l, \psi(\rho_l)) + \mathcal{R}(\psi(\rho_l), \rho_r) & \text{if } \rho_r < \psi(\rho_l) \\ \mathcal{NS}(\rho_l, \rho_r) & \text{if } \rho_r \geq \psi(\rho_l) \end{cases}$$

- Otherwise, $\mathcal{R}_{NC}(\rho_l, \rho_r) = \mathcal{R}(\rho_l, \rho_r)$.

4.1 The constrained nonclassical Riemann solver

As in Section 2.1, we construct the constrained Riemann solver derived from $\mathcal{R}_{NC}$.

Definition 4.1 *A Riemann solver $\mathcal{R}^F_{NC} : (\rho_l, \rho_r) \mapsto \mathcal{R}^F_{NC}(\rho_l, \rho_r)$ for (1.1)-(1.3) is defined as follows.*
If $f\left(\mathcal{R}_{NC}(\rho_l, \rho_r)(0)\right) \leq F$, then $\mathcal{R}^F_{NC}(\rho_l, \rho_r) = \mathcal{R}_{NC}(\rho_l, \rho_r)$.
Otherwise, if $s < \rho_l < R$ and $\hat{\rho}^F_l > \rho_l + \Delta s$ then

$$\mathcal{R}^F_{NC}(\rho_l, \rho_r)(\lambda) = \begin{cases} \mathcal{R}_{NC}(\rho_l, \hat{R}^{*F}_M)(\lambda) \ \textit{if } \lambda < 0\,, \\ \mathcal{R}_{NC}(\check{\rho}^F_r, \rho_r)(\lambda) \ \textit{if } \lambda > 0\,. \end{cases}$$

In all the other cases

$$\mathcal{R}^F_{NC}(\rho_l, \rho_r)(\lambda) = \begin{cases} \mathcal{R}_{NC}(\rho_l, \hat{\rho}^F_l)(\lambda) \ \textit{if } \lambda < 0\,, \\ \mathcal{R}_{NC}(\check{\rho}^F_r, \rho_r)(\lambda) \ \textit{if } \lambda > 0\,. \end{cases}$$

In order to check that the above definition is correct, observe first of all that if $f(\rho_l) \leq F$, then $\hat{\rho}^F_l \leq \rho_l$ and consequently $\mathcal{R}_{NC}(\rho_l, \hat{\rho}^F_l) = \mathcal{R}(\rho_l, \hat{\rho}^F_l)$ and we fa ll in the setting of Definition 2.1. Similarly, if $f(\rho_r) \leq F$, then $\check{\rho}^F_r \geq \rho_r$ and consequently $\mathcal{R}_{NC}(\check{\rho}^F_r, \rho_r) = \mathcal{R}(\check{\rho}^F_r, \rho_r)$

Consider now the case $f(\rho_l) > F$. We have to distinguish three cases:

- If $F \in]f(R^*_M), f(R_M)]$, then $\mathcal{R}_{NC}(\rho_l, \hat{\rho}^F_l) = \mathcal{R}(\rho_l, \hat{\rho}^F_l)$.
- If $F \in [f(R), f(R^*_M)]$, and moreover $\rho_l > s$, $\hat{\rho}^F_l > \rho_l + \Delta s$, then $\mathcal{R}_{NC}(\rho_l, \hat{\rho}^F_l)$ would contain positive waves, and would not satisfy the constraint (2.7). On the contrary, $\mathcal{R}_{NC}(\rho_l, \hat{R}^{*F}_M) = \mathcal{NS}(\rho_l, \hat{R}^{*F}_M)$ consists of a shock with negative speed. In all the other cases $\mathcal{R}_{NC}(\rho_l, \hat{\rho}^F_l) = \mathcal{R}(\rho_l, \hat{\rho}^F_l)$.

- If $F \in [0, f(R)[$, $\mathcal{R}_{NC}(\rho_l, \hat{\rho}_l^F)$ contains only waves with negative speeds.

We now check the right hand side of the Riemann solver, i.e. for $\lambda > 0$, and $f(\rho_r) > F$. We distinguish two cases:

- If $F \in [f(R), f(R_M)]$, then $\mathcal{R}_{NC}(\check{\rho}_r^F, \rho_r) = \mathcal{R}(\check{\rho}_r^F, \rho_r)$.
- If $F \in [0, f(R)[$, then $\mathcal{R}_{NC}(\check{\rho}_r^F, \rho_r)$ contains only waves with positive speeds.

Notice that nonclassical shocks can appear both in $\mathcal{R}_{NC}(\rho_l, \hat{\rho}_l^F)$ and $\mathcal{R}_{NC}(\check{\rho}_r^F, \rho_r)$ as, for example, if $F < f(R)$, $\rho_l \in [0, R_M]$ with $f(\rho_l) > F$ and $\rho_r \in [R, R_M^*]$ (which implies $f(\rho_r) > F$).

5 Application to pedestrian flow modeling

Following [10, 13], we consider a corridor modeled by the segment $[0, L]$, with an exit at $x = D$, with $0 < D < L$. Then, the dynamics of the crowd exiting the corridor is described by (1.1)-(1.3), with the Riemann solver described in Section 4. In emergency situations, it is well known that the pressure of the people seeking to exit may dramatically reduce the door efficiency. To prevent this, suitable obstacles (such as columns) can be posed before the exit to reduce the crowd pressure. Paradoxically, the insertion of obstacles may reduce the evacuation time, although most individuals may have a slightly longer path to reach the exit. This remarkable behavior mimics the Braess paradox [2] typical of networks and is captured by the model considered here.

We assume that a group of people is uniformly distributed on the segment $[a, b]$, with $0 < a < b < D$, and an obstacle is placed at $x = d$, with $b < d < D$, see Figure 3.

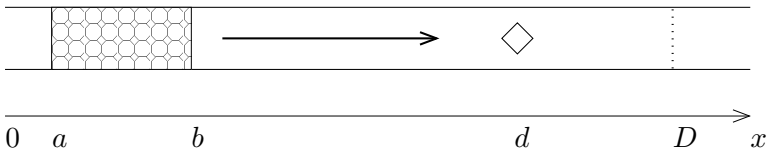

Figure 3: A corridor with an obstacle before the exit.

The dynamic of the crowd is then described by

$$\begin{cases} \partial_t \rho + \partial_x f(\rho) = 0 & f\left(\rho(t, d-)\right) \leq q\left(\rho(t, d-)\right), \\ \rho(0, x) = \rho_o(x) & f\left(\rho(t, D-)\right) \leq Q\left(\rho(t, D-)\right). \end{cases} \tag{5.1}$$

Since the efficiency of the exit is reduced when the crowd is panicking, we assume that

$$\begin{aligned} q(\rho) &= \begin{cases} \hat{q} & \text{if} \quad \rho \in [0, R] \\ \check{q} & \text{if} \quad \rho \in]R, R^*] \end{cases} \qquad \text{with} \quad \hat{q} > \check{q}, \\ Q(\rho) &= \begin{cases} \hat{Q} & \text{if} \quad \rho \in [0, R] \\ \check{Q} & \text{if} \quad \rho \in]R, R^*] \end{cases} \qquad \text{with} \quad \hat{Q} > \check{Q}. \end{aligned} \tag{5.2}$$

Aiming at pedestrian flow management and exits design, the evacuation time T is particularly relevant and can be computed integrating (5.1)–(5.2) numerically following the procedure described in Sections 5.1 and 5.2 below. If the initial datum is particularly simple, i.e. constant on a given segment, an analytical study is also possible, see Figure 4. The detailed construction

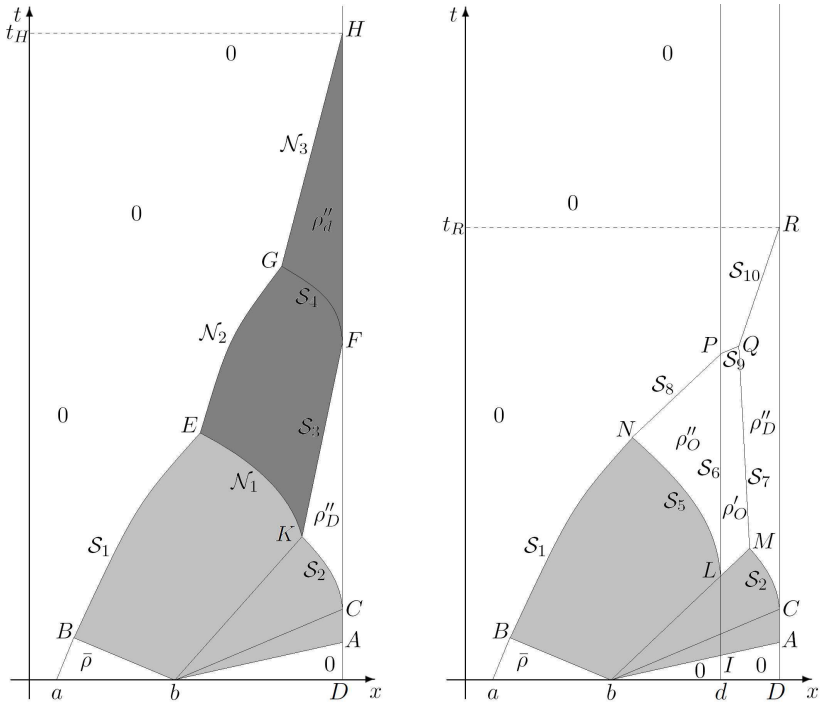

Figure 4: Wave-front tracking applied to (5.1)–(5.2). Left, the structure of the solution without obstacle ($q \geq \max(f(\rho))$): the evacuation time is t_H. Right, in the presence of the obstacle, the evacuation time is $t_R < t_H$. (Taken from [10, 13].)

of these solutions can be found in [13, Section 4.2]. Note that the darker regions in Figure 4, left, represent the regions where the crowd density attains panic values, i.e. $\rho \in]R, R^*]$. The presence of the obstacle avoids the density to reach panic regimes, thus allowing for a faster evacuation from the room.

5.1 A numerical scheme for classical and nonclassical solutions

The numerical scheme we propose here for computing classical and nonclassical solutions of (1.1)-(1.2) follows the same "sharp-interface approach" as in [5, 6]. It is made of two steps. The first step tracks the (classical or nonclassical) discontinuities arising in the Riemann problems set at the mesh interfaces. The second step consists of a random sampling strategy in order to avoid dealing with moving meshes.

Let us first define the set $\mathcal{N} \in [0, R^*]^2$ made of the pairs (ρ_l, ρ_r) such that the nonclassical Riemann solution $\mathcal{R}_{NC}(\rho_l, \rho_r)$ is actually nonclassical, that is to say contains a nonclassical shock. Similarly, we define the set $\mathcal{C} \in [0, R^*]^2$ made of the pairs (ρ_l, ρ_r) such that the Riemann solution $\mathcal{R}_{NC}(\rho_l, \rho_r)$ is classical and contains a (classical) shock. (See Fig. 2, right.)

Let us now present the numerical scheme for classical and nonclassical solutions. We keep the notation of section 3 and, being given the sequence $(\rho_j^n)_{j\in\mathbb{Z}}$ at time t^n, the point is now to propose a definition of $(\rho_j^{n+1})_{j\in\mathbb{Z}}$ by a recurrence relation.

Step 1 : Tracking the discontinuities and averaging ($t^n \to t^{n+1-}$)

The idea of this step is to first track the nonclassical or classical discontinuities in the Riemann problems set at each mesh interface, and then to average the solution on both sides of these discontinuities.

As is customary in the classical Godunov method, one first solves theoretically the Cauchy problem (1.1)-(1.2) with $\rho_0(x) = \rho_\nu(x, t^n)$ for times $t \in [0, \Delta t]$. Under the usual CFL restriction

$$\frac{\Delta t}{\Delta x} \max_\rho\{|f'(\rho)|\} \leq \frac{1}{2}, \tag{5.3}$$

for all the ρ under consideration, the solution is known by gluing together the solutions of the Riemann problems set at each interface. More precisely

$$\rho(x,t) = \rho_{\mathbf{r}}(\frac{x - x_{j+1/2}}{t}; \rho_j^n, \rho_{j+1}^n) \text{ for all } (x,t) \in [x_j, x_{j+1}] \times [0, \Delta t], \tag{5.4}$$

where $x_j = \frac{x_{j-1/2}+x_{j+1/2}}{2}$ and $(x,t) \to \rho_{\mathbf{r}}(\frac{x}{t}; \rho_l, \rho_r)$ denotes the Riemann solution $\mathcal{R}_{NC}(\rho_l, \rho_r)$.

In order to track the discontinuities, we then define the sequence $(\sigma_{j+1/2}^n = \sigma(\rho_j^n, \rho_{j+1}^n))_{j\in\mathbb{Z}}$ of characteristic speeds of propagation at interfaces $(x_{j+1/2})_{j\in\mathbb{Z}}$ as follows :

- if (ρ_j^n, ρ_{j+1}^n) belongs to $\mathcal{N}$, then $\sigma_{j+1/2}^n$ coincides with the speed of propagation of the nonclassical discontinuity in the Riemann solution $\mathcal{R}_{NC}(\rho_j^n, \rho_{j+1}^n)$;
- if (ρ_j^n, ρ_{j+1}^n) belongs to $\mathcal{C}$, then $\sigma_{j+1/2}^n$ coincides with the speed of propagation of the classical discontinuity in the Riemann solution $\mathcal{R}_{NC}(\rho_j^n, \rho_{j+1}^n)$, if any;
- otherwise, $\sigma_{j+1/2}^n = 0$.

Assuming for all $j \in \mathbb{Z}$ that the interface $x_{j+1/2}$ moves at velocity $\sigma_{j+1/2}^n$ between times t^n and $t^{n+1} = t^n + \Delta t$, it is natural to define the new interface $\overline{x}_{j+1/2}^n$ at time t^{n+1} by

$$\overline{x}_{j+1/2}^n = x_{j+1/2} + \sigma_{j+1/2}^n \, \Delta t, \quad j \in \mathbb{Z}. \tag{5.5}$$

We also introduce the notation $\overline{\Delta x}_j^n = \overline{x}_{j+1/2}^n - \overline{x}_{j-1/2}^n$, $j \in \mathbb{Z}$.
At last, averaging the solution on $\overline{\mathcal{C}}_j^n$ provides us with a piecewise constant approximate solution $\overline{\rho}_\nu(x, t^{n+1-})$ on a non uniform mesh defined by

$$\overline{\rho}_\nu(x, t^{n+1-}) = \overline{\rho}_j^{n+1-} \text{ for all } x \in \overline{C}_j^n, \ j \in \mathbb{Z}, \ n \in \mathbb{N},$$

with

$$\overline{\rho}_j^{n+1-} = \frac{1}{\overline{\Delta x}_j^n} \int_{\overline{x}_{j-1/2}^n}^{\overline{x}_{j+1/2}^n} \rho(x, \Delta t) dt, \ j \in \mathbb{Z}.$$

It is worth noticing that the modified cells $\overline{\mathcal{C}}_j^n$ may be either smaller or larger than the original ones $\mathcal{C}_j$, depending on the signs of the velocities $\sigma_{j+1/2}^n$, $j \in \mathbb{Z}$. This is illustrated on Figures 5 and 6 below.

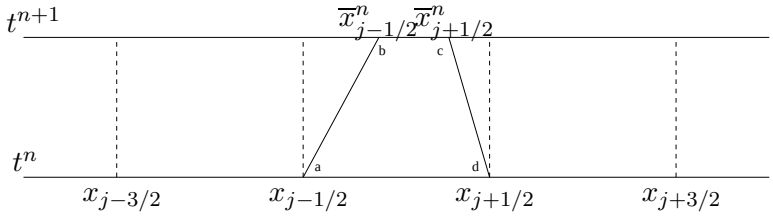

Figure 5: A first example of modified cells tracking the discontinuities.

Actually, using notations introduced on Figures 5 and 6 and integrating (1.1) over the element $\overline{E} = (abcd)$ with use of Green's theorem, we classically obtain the simpler formula

$$\overline{\rho}_j^{n+1-} = \frac{\Delta x}{\overline{\Delta x}_j^n} \rho_j^n - \frac{\Delta t}{\overline{\Delta x}_j^n} (\overline{\mathbf{f}}_{j+1/2}^{n,-} - \overline{\mathbf{f}}_{j-1/2}^{n,+}) \text{ for all } j \in \mathbb{Z}. \tag{5.6}$$

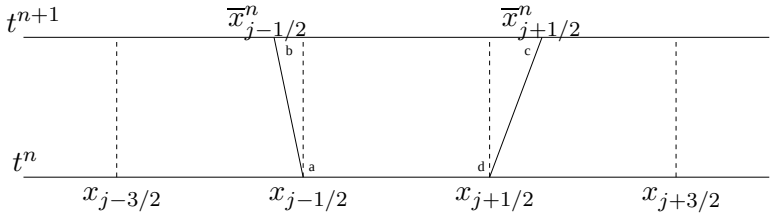

Figure 6: A second example of modified cells tracking the discontinuities.

The numerical fluxes are defined by

$$\overline{f}^{n,\pm}_{j+1/2} = f(\rho_{\mathbf{r}}(\sigma^{n,\pm}_{j+1/2};\rho^n_j,\rho^n_{j+1})) - \sigma^n_{j+1/2}\rho_{\mathbf{r}}(\sigma^{n,\pm}_{j+1/2};\rho^n_j,\rho^n_{j+1}) \text{ for all } j \in \mathbb{Z}, \tag{5.7}$$

where we have used the usual notations $\sigma^{n,\pm}_{j+1/2}$ to denote the left and right traces of the Riemann solutions at points $\sigma^n_{j+1/2}$.

Remark. The conservation property

$$\begin{array}{c} f(\rho_{\mathbf{r}}(\sigma^{n,-}_{j+1/2};\rho^n_j,\rho^n_{j+1})) - \sigma^n_{j+1/2}\rho_{\mathbf{r}}(\sigma^{n,-}_{j+1/2};\rho^n_j,\rho^n_{j+1}) \\ = \\ f(\rho_{\mathbf{r}}(\sigma^{n,+}_{j+1/2};\rho^n_j,\rho^n_{j+1})) - \sigma^n_{j+1/2}\rho_{\mathbf{r}}(\sigma^{n,+}_{j+1/2};\rho^n_j,\rho^n_{j+1}) \end{array} \tag{5.8}$$

remains valid thanks to Rankine-Hugoniot conditions.

We finally introduce the notation $\overline{f}^{\pm}(\rho^n_j,\rho^n_{j+1}) = \overline{f}^{n,\pm}_{j+1/2}$ for the numerical fluxes, with of course

$$\overline{f}^{\pm}(\rho^n_j,\rho^n_{j+1}) \;=\; f(\rho_{\mathbf{r}}(\sigma^{n,\pm}_{j+1/2};\rho^n_j,\rho^n_{j+1})) - \sigma^n_{j+1/2}\rho_{\mathbf{r}}(\sigma^{n,\pm}_{j+1/2};\rho^n_j,\rho^n_{j+1}). \tag{5.9}$$

Recall that $\sigma^n_{j+1/2} = \sigma(\rho^n_j,\rho^n_{j+1})$ by definition.

To conclude this first step, let us emphasize that when the Riemann solution between ρ^n_j and ρ^n_{j+1} does not present discontinuities, then $\sigma^n_{j+1/2} = 0$ and the numerical fluxes $\overline{f}^{n,\pm}_{j+1/2}$ coincide with the usual numerical flux

$$\overline{f}(\rho^n_j,\rho^n_{j+1}) = f(\rho_{\mathbf{r}}(0;\rho^n_j,\rho^n_{j+1}))$$

associated with the Godunov method. This numerical flux may of course be replaced by any consistent numerical flux for the sake of simplicity. In the proposed numerical simulation below, we replaced for instance this Godunov numerical flux by the Rusanov numerical flux as soon as the solution joining ρ^n_j to ρ^n_{j+1} does not display discontinuities. This amounts to set

$$\overline{f}(\rho^n_j,\rho^n_{j+1}) = \frac{1}{2}(f(\rho^n_j) + f(\rho^n_{j+1}) - \alpha_{j+1/2}(\rho^n_{j+1} - \rho^n_j)), \tag{5.10}$$

with

$$\alpha_{j+1/2} = \max\left(f'(\rho_j^n), f'(\rho_{j+1}^n)\right).$$

Step 2 : Random sampling ($t^{n+1-} \to t^{n+1}$)

In order to avoid dealing with moving meshes, we propose to define the new approximation ρ_j^{n+1} at time t^{n+1} on the (uniform) cells $\mathcal{C}_j$, $j \in \mathbb{Z}$ using a random sampling strategy. More precisely, we propose to pick up randomly a value between $\overline{\rho}_{j-1}^{n+1-}$, $\overline{\rho}_j^{n+1-}$ and $\overline{\rho}_{j+1}^{n+1-}$, according to their rate of presence in the cell $\mathcal{C}_j$. Given a well distributed random sequence (a_n) in interval $(0,1)$, it leads to set:

$$\rho_j^{n+1} = \begin{cases} \overline{\rho}_{j-1}^{n+1-} & \text{if} \quad a_{n+1} \in (0, \frac{\Delta t}{\Delta x}\max(\sigma_{j-1/2}^n, 0)), \\ \overline{\rho}_j^{n+1-} & \text{if} \quad a_{n+1} \in [\frac{\Delta t}{\Delta x}\max(\sigma_{j-1/2}^n, 0), 1 + \frac{\Delta t}{\Delta x}\min(\sigma_{j+1/2}^n, 0)), \\ \overline{\rho}_{j+1}^{n+1-} & \text{if} \quad a_{n+1} \in [1 + \frac{\Delta t}{\Delta x}\min(\sigma_{j+1/2}^n, 0), 1), \end{cases} \tag{5.11}$$

for all $j \in \mathbb{Z}$.
Following Colella [8], we consider in practice the low-discrepancy van der Corput random sequence (a_n) defined by

$$a_n = \sum_{k=0}^{m} i_k 2^{-(k+1)},$$

where $n = \sum_{k=0}^{m} i_k 2^k$, $i_k = 0, 1$, denotes the binary expansion of the integers $n = 1, 2, \ldots$. This concludes the description of the modified Godunov scheme.

To conclude this section, it is worth emphasizing that due to the sampling procedure, the proposed algorithm is not strictly conservative in the classical sense of finite volumes methods. However, we observed (see also for instance [5, 6]) that this drawback does not prevent the solution to converge to the right one. In particular, discontinuities propagate with the right speed and conservation errors tend to zero with the mesh size. On the other hand, it is easily seen that if we focus on initial data leading to a solution that consists of an isolated (classical or nonclassical) discontinuity, the proposed method coincides with the Glimm's random choice scheme and then converges to the exact solution.

5.2 A numerical scheme for constrained classical and nonclassical solutions

We propose to describe in this section how to deal with constrained solutions. In practice and as motivated in the previous section, such constraints will appear at the exit of a corridor and possibly at suitable obstacles like

columns posed before the exit of the corridor in order to lessen the crowd pressure. In this paragraph, we denote by $x_{j_c+1/2} = (j_c + 1/2)\Delta x$ the mesh interface associated with the position where such a constraint takes place (that is typically the position of the exit or of an obstacle).

In the frame of the numerical scheme proposed for non-constrained classical and nonclassical solutions in the previous subsection, it is a matter of defining $\sigma^n_{j_c+1/2}$ and the corresponding numerical fluxes $\overline{f}^{n,\pm}_{j_c+1/2} = \overline{f}^{\pm}(\rho^n_{j_c}, \rho^n_{j_c+1})$.

Following [1], we propose to set $\sigma^n_{j_c+1/2} = 0$ and to naturally define the numerical flux at the interface $x_{(j_c+1/2)}$ as in Section 3 by the following constrained formula

$$\overline{f}^{\pm}(\rho^n_{j_c}, \rho^n_{j_c+1}) = \min\left(\overline{f}(\rho^n_{j_c}, \rho^n_{j_c+1}), F\right)$$

where F represents the flux constraint and $\overline{f}(\rho^n_{j_c}, \rho^n_{j_c+1})$ is given by the Rusanov formula (5.10).
There are thus two possibilities. The first one corresponds to the non-constrained situation $\overline{f}^{\pm}(\rho^n_{j_c}, \rho^n_{j_c+1}) < F$, where we use the classical Rusanov numerical flux. The second one corresponds to the constrained situation $\overline{f}^{\pm}(\rho^n_{j_c}, \rho^n_{j_c+1}) = F$. In that case, the numerical flux is given by the constraint itself. From the theoretical point of view, a stationary discontinuity is expected to take place between the left and right states given by $(\hat{\rho}^{nF}_{j_c}, \check{\rho}^{nF}_{j_c+1})$ in the classical case, and in the nonclassical case by $(\hat{R}^{*F}_M, \check{\rho}^{nF}_{j_c+1})$ (if $s < \rho^n_{j_c} < R$ and $\hat{\rho}^{nF}_{j_c} > \rho^n_{j_c} + \Delta s$) or $(\hat{\rho}^{nF}_{j_c}, \check{\rho}^{nF}_{j_c+1})$ otherwise, see Definitions 2.1 and 4.1 of the constrained classical and nonclassical Riemann solvers. To avoid cumbersome notations, we denote by $(\rho^-_{j_c+1/2}, \rho^+_{j_c+1/2})$ these left and right states.

In order to take into account this theoretical statement at the numerical level, we also propose to modify the definition of the numerical fluxes $\overline{f}^{n,\pm}_{j_c-1/2}$ and $\overline{f}^{n,\pm}_{j_c+3/2}$ by setting

$$\overline{f}^{n,\pm}_{j_c-1/2} = \overline{f}^{\pm}(\rho^n_{j_c-1}, \rho^-_{j_c+1/2})$$

and

$$\overline{f}^{n,\pm}_{j_c+3/2} = \overline{f}^{\pm}(\rho^+_{j_c+1/2}, \rho^n_{j_c+2}),$$

with $\overline{f}^{\pm}(.,.)$ defined above by (5.9).

5.3 Numerical experiment and Braess paradox

As an illustrative simulation, we perform the so-called Braess paradox numerical experiment described in the early section. Let us begin with the

simulation parameters. We have considered the flow function [13, Section 4.3]

$$f(\rho) = \max\left\{\frac{\rho(7-\rho)}{6}, \frac{3(\rho-6)(2\rho-21)}{20(\rho-12)}\right\},$$

whose diagram is given in Figure 1 (left), leading to

$$R \approx 6.842786, \quad R^* = 10.5.$$

The nonclassical Riemann solver parameters are given by

$$s = 1.2, \quad \Delta_s = 5.6.$$

The computational domain modeling the corridor corresponds to the interval $[0, L]$ with $L = 3.6$, and the the exit is located at $x = D$ with $D = 3.1$. The position of the obstacle (when present) is 2.45. The initial data is chosen to be

$$\rho_0(x) = \begin{cases} 0 & \text{if} \quad x < a = 0.1 \quad \text{and} \quad x > b = 1.1 \\ 5.3 & \text{if} \quad a < x < b, \end{cases}$$

and is represented on Figure 7 below. The constraint functions q and Q in

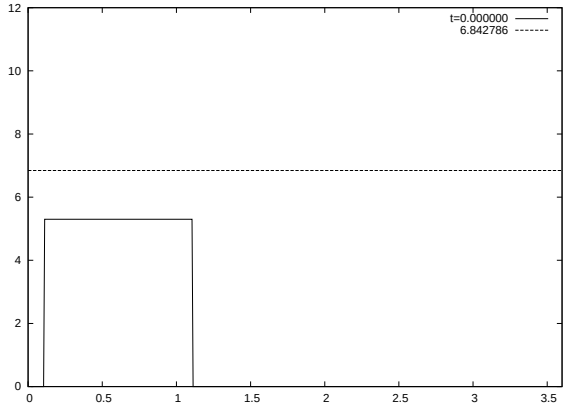

Figure 7: Braess paradox simulation : initial data

(5.2) are considered with the following parameters :

$$\hat{q} = 1, \quad \hat{Q} = 0.2, \quad \check{Q} = 0.1793.$$

Note that the constraint function q is not active when the obstacle is not present while the parameter $\check{q}$ entering its definition does not play any role since no panic will be observed at the obstacle position. Note also that, from a numerical point of view, these flux constraints are imposed at both interfaces $j_c + 1/2$ associated with the obstacle and exit positions. The left traces $d-$ and $D-$ of the density in (5.1) are then naturally considered to be ρ_{j_c}.

We show here the results of two simulations, one without obstacle and one with obstacle, where we used a 500-point mesh and a CFL condition equal to 0.5. We propose on Figure 8 four snapshots of each numerical solution. The numerical results without obstacle are depicted on the left side and we clearly see on the second picture that panic arises as expected since the density gets greater than R near the exit position. The numerical exit time is 28.833. On the contrary, no panic is created when the obstacle is present and the computed exit time now equals 24.883.

6 Proofs

6.1 Proof of Lemma 2.6

(i) We want to check that

$$\forall (c_l, c_r), (b_l, b_r) \in \mathcal{G}(F) \quad \Phi(c_l, b_l) \geq \Phi(c_r, b_r). \tag{6.1}$$

- If $(c_l, c_r), (b_l, b_r) \in \mathcal{G}_1(F)$, then $f(c_l) = f(c_r) = f(b_l) = f(b_r) = F$ and $\Phi(c_l, b_l) = 0 = \Phi(c_r, b_r)$.
- If $(c^l, c^r) \in \mathcal{G}_1(F)$, $(b^l, b^r) \in \mathcal{G}_2(F)$ (then $b_l = b_r = b$ and $f(b) \leq F$). In this case, either $F \in [0, f(r)[\cup]f(R_M^*), f(R_M)]$ and $\mathcal{G}_1(F) = \left\{(\rho_2^F, \rho_1^F)\right\}$, or $F \in [f(r), f(R_M^*)]$ and

  $$\mathcal{G}_1(F) = \left\{(\rho_4^F, \rho_1^F), (\rho_4^F, \rho_2^F), (\rho_4^F, \rho_3^F), (\rho_3^F, \rho_1^F), (\rho_2^F, \rho_1^F)\right\}.$$

  We have to check several cases. If $b \leq \rho_1^F$, then

  $$\Phi(c_l, b) - \Phi(c_r, b) = f(c_l) - f(b) - f(c_r) + f(b) = 0.$$

  If $b \geq \max_i\{\rho_i^F\}$, then again

  $$\Phi(c_l, b) - \Phi(c_r, b) = f(b) - f(c_l) - f(b) + f(c_r) = 0.$$

  If $\rho_2^F < b < \rho_3^F$, then we may have $c_r < b < c_l$ and

  $$\Phi(c_l, b) - \Phi(c_r, b) = f(c_l) - f(b) - f(b) + f(c_r) = 2F - 2f(b) \geq 0.$$

- If $(c_l, c_r) \in \mathcal{G}_1(F)$, $(b_l, b_r) \in \mathcal{G}_3(F)$, then we can face several situations. If $b_l \leq c_r < c_l \leq b_r$, then

  $$\Phi(c_l, b_l) - \Phi(c_r, b_r) = f(c_l) - f(b_l) - f(b_r) + f(c_r) = 2F - 2f(b_{l,r}) \geq 0.$$

  If $b_l, b_r \leq c_r < c_l$, then

  $$\Phi(c_l, b_l) - \Phi(c_r, b_r) = f(c_l) - f(b_l) - f(c_r) + f(b_r) = 0.$$

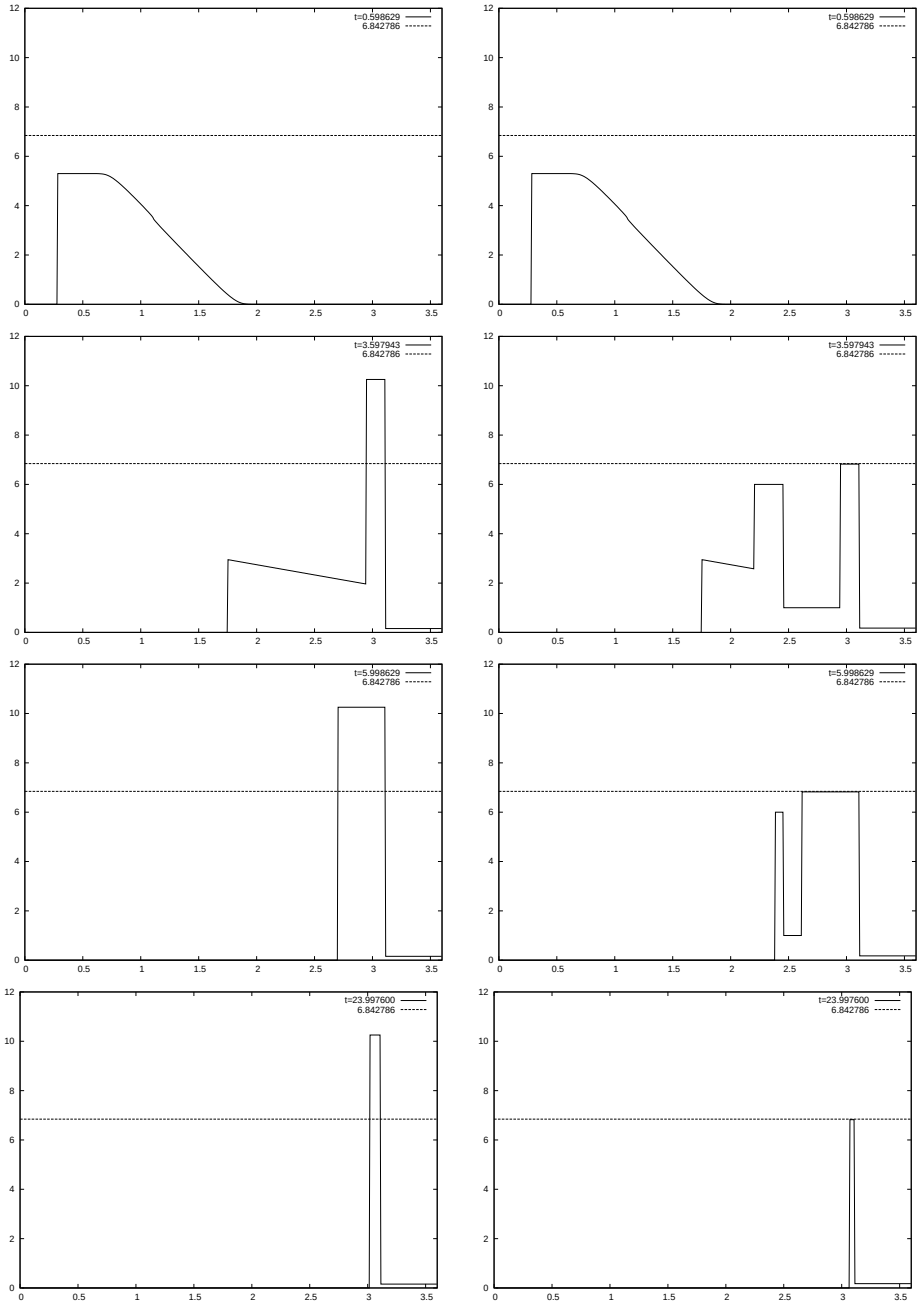

Figure 8: Braess paradox simulation : without obstacle (left) and with obstacle (right)

If $b_l, b_r \geq c_l > c_r$, then

$$\Phi(c_l, b_l) - \Phi(c_r, b_r) = f(b_l) - f(c_l) - f(b_r) + f(c_r) = 0.$$

Finally, if $c_r \leq b_r < b_l \leq c_l$, then

$$\Phi(c_l, b_l) - \Phi(c_r, b_r) = f(c_l) - f(b_l) - f(b_r) + f(c_r) = 2F - 2f(b_{l,r}) \geq 0.$$

- If $(c_l, c_r), (b_l, b_r) \in \mathcal{G}_2(F) \cup \mathcal{G}_3(F)$, then the pairs (b_l, b_r), (c_l, c_r) correspond to the Kruzhkov stationary solutions

  $$\tilde{b}(t,x) := b_l \mathbb{1}_{\{x<0\}} + b_r \mathbb{1}_{\{x>0\}}, \quad \tilde{c}(t,x) := c_l \mathbb{1}_{\{x<0\}} + c_r \mathbb{1}_{\{x>0\}}$$

  of the conservation law (1.1); inequality $\Phi(c_l, b_l) - \Phi(c_r, b_r) \geq 0$ is well known in this context (see [24]).

The remaining cases are deduced by symmetry of Φ; this proves (6.1).

(ii) Let us reason by contradiction. If $f(b_l) = f(b_r)$ but $(b_l, b_r) \notin \mathcal{G}(F)$, then either $f(b_{l,r}) > F$, or $f(b_{l,r}) < F$ and there exists $b^* \in [b_l \perp b_r, b_l \top b_r]$ such that $(b^* - b_l)(f(b^*) - f(b_l)) < 0$. In the first case, we can take $c_r < b_{l,r} < c_l$, then

$$\Phi(c_l, b_l) - \Phi(c_r, b_r) = f(c_l) - f(b_l) - f(b_r) + f(c_r) = 2F - 2f(b_{l,r}) < 0.$$

In the second case, we distinguish two subcases. If $b_r < b_l$, we can take $b_r < c_r \leq c_l < b_l$, and we get

$$\Phi(c_l, b_l) - \Phi(c_r, b_r) = f(b_l) - f(c_l) - f(c_r) + f(b_r) = 2f(b_{l,r}) - 2F < 0.$$

If $b_r > b_l$, we take $c_l = c_r = b^* \in]b_l, b_r[$ and we get

$$\Phi(b^*, b_l) - \Phi(b^*, b_r) = f(b^*) - f(b_l) - f(b_r) + f(b^*) = 2f(b^*) - 2f(b_{l,r}) < 0.$$

Thus in all the cases, we arrive to a contradiction with assumption (2.13).

6.2 Proof of Theorem 2.7

Due to the constraint (1.3), one cannot hope to find an uniform bound of the total variation of approximate solutions constructed by wave-front tracking (or any other approximating technique). To overcome this difficulty, we introduce an extension to the usual Temple functional [23]. Let $\rho_1, \ldots, \rho_N \in]0, R[$ be the points of local minima or maxima of f, set $\rho_0 = 0$, $\rho_{N+1} = R$, and define for $i = 1, \ldots, N+1$

$$\Psi(\rho) = \sum_{j=0}^{i-1} \big|f(\rho_j) - f(\rho_{j-1})\big| + \big|f(\rho) - f(\rho_{i-1})\big|, \quad \text{if } \rho \in [\rho_{i-1}, \rho_i[. \quad (6.2)$$

(Recall that under hypotheses **(F.2)**-**(F.5)** we have $N = 3$ and $\rho_1 = R_M$, $\rho_2 = r$ and $\rho_3 = R_M^*$.) We now follow the procedure in [9, § 4.2]. Fix a positive $n \in \mathbb{N}$, $n > 0$, and introduce in $[0, R]$ the mesh $\mathcal{M}_n$ by $\mathcal{M}_n = f^{-1}(2^{-n}\mathbb{N}) \cup \{\rho_1, \dots, \rho_N\}$. Let $\mathbf{PLC}_n$ be the set of piecewise linear and continuous functions defined on $[0, R]$ whose derivatives exist in $]0, R[\backslash\mathcal{M}_n$. Let $f^n \in \mathbf{PLC}_n$ coincide with f on $\mathcal{M}_n$.

Similarly, introduce $\mathbf{PC}_n$, respectively $\mathbf{PC}_n^+$, as the set of piecewise constant functions defined on $\mathbb{R}$, respectively $\mathbb{R}^+$, with values in $\mathcal{M}_n$, respectively in $f(\mathcal{M}_n)$. Let $F^n \in \mathbf{PC}_n^+$, coincide with F on $f(\mathcal{M}_n)$, in the sense that $F(t) = F^n(t)$ whenever $F(t) \in f(\mathcal{M}_n)$. We write

$$\begin{array}{rcll} \rho^n & = & \displaystyle\sum_{\alpha\geq 1} \rho_\alpha^n \, \chi_{]x_{\alpha-1}, x_\alpha]} & \text{with } \rho_\alpha^n \in \mathcal{M}_n \\ F^n & = & F_0^n \, \chi_{[0,t_1]} + \displaystyle\sum_{\beta\geq 1} F_\beta^n \, \chi_{]t_\beta, t_{\beta+1}]} & \text{with } F_\beta^n \in f(\mathcal{M}_n) \end{array} \tag{6.3}$$

and we agree that for $\alpha = 0$, $x_\alpha = 0$. Both the approximations above are meant in the strong $\mathbf{L^1}$ topology, that is

$$\lim_{n\to+\infty} \Big(\|\rho^n - \rho\|_{\mathbf{L^1}(\mathbb{R};\mathbb{R})} + \|F^n - F\|_{\mathbf{L^1}(\mathbb{R}^+;\mathbb{R})} \Big) = 0 \,.$$

Let $\mathcal{D}_n = \big\{\rho \in \mathbf{PC}_n \colon \Psi(\rho) \in \mathbf{BV}(\mathbb{R};\mathbb{R})\big\}$ and $\bar{\mathcal{D}}_n = \mathcal{D}_n \times \mathbf{PC}_n^+$. On any $(\rho^n, F^n) \in \bar{\mathcal{D}}_n$, written as in (6.3), define the Glimm type functional

$$\Upsilon(\rho^n, F^n) = \sum_\alpha \big|\Psi(\rho_{\alpha+1}^n) - \Psi(\rho_\alpha^n)\big| + 5 \sum_{t_\beta \geq 0} \Big|F_{\beta+1}^n - F_\beta^n\Big| + \gamma \,, \tag{6.4}$$

where γ is defined as follows. Let $\mathcal{G}_1(F)$ be decomposed in the subsets:

$$\begin{array}{rcl} \mathcal{G}_1^a(F) & = & \big\{(c_l, c_r) \in \mathcal{G}_1(F) : c_l > R_M^*,\ c_r < R_M\big\} \,, \\ \mathcal{G}_1^b(F) & = & \big\{(c_l, c_r) \in \mathcal{G}_1(F) : c_l > R_M^*,\ R_M < c_r < R_m^*\big\} \,, \\ \mathcal{G}_1^c(F) & = & \big\{(c_l, c_r) \in \mathcal{G}_1(F) : R_M < c_l < R_M^*,\ c_r < R_M\big\} \,. \end{array}$$

Then, if $F^n(0) < f(r)$,

$$\gamma = 0 \,, \qquad \text{if } (\rho^n(0-), \rho^n(0+)) \in \mathcal{G}_1(F^n(0)) \,;$$

if $F^n(0) \geq f(r)$,

$$\gamma = \begin{cases} \gamma_a = 4\big(F^n(0) - f(r)\big) \,, & \text{if } (\rho^n(0-), \rho^n(0+)) \in \mathcal{G}_1^a(F^n(0)) \,, \\ \gamma_b = 4\big(f(R_M) - f(r)\big) \,, & \text{if } (\rho^n(0-), \rho^n(0+)) \in \mathcal{G}_1^b(F^n(0)) \,, \\ \gamma_c = 4\big(f(R_M^*) - f(r)\big) \,, & \text{if } (\rho^n(0-), \rho^n(0+)) \in \mathcal{G}_1^c(F^n(0)) \,; \end{cases}$$

otherwise

$$\gamma = \gamma_o = 4\big(f(R_M) - f(r) + f(R_M^*) - F^n(0)\big) \,.$$

Observe that $0 \leq \gamma \leq \gamma_o$.

We then follow the nowadays classical wave-front tracking technique which dates back to [15], see also [3, § 6], or [9] for the constrained case. At any interaction, the functional Υ either decreases by at least 2^{-n}, or remains constant with the total number of waves in the approximate solution that does not increase (see Appendix for details).

A standard application of Helly's Theorem, see [3, Theorem 2.4], yields the existence of a subsequence of approximate solutions, still denoted by ρ^n, converging in $\mathbf{L^1}_{loc}(\mathbb{R}^+ \times \mathbb{R})$ to a solution u of (1.1)-(1.3) in the sense of Definitions 2.2. In fact, the entropy inequality (2.6) is easily recovered by passing to the limit in the approximate solutions. In order to verify the constraint (2.7), we consider the weak formulation of (1.1) in the half-domain $\mathbb{R}^+ \times \mathbb{R}^+$ ($\mathbb{R}^+ \times \mathbb{R}^-$ respectively), which gives us, for all $\varphi \in \mathbf{C_c^1}(\mathbb{R}^+ \times \mathbb{R}; \mathbb{R}^+)$,

$$\begin{aligned}\int_0^\infty \int_0^\infty \left(\rho^n \partial_t \varphi + f(\rho^n)\partial_x \varphi\right) dx\ dt &= \int_0^\infty \gamma_w(f(\rho^n))(t,0+)\varphi(t,0)\ dt \\ &= \int_0^\infty f(\rho^n(t,0+))\ \varphi(t,0)\ dt \\ &\leq \int_0^\infty F^n(t)\ \varphi(t,0)\ dt\end{aligned}$$

where $\gamma_w(f(\rho^n))(t)$ are the weak normal traces of the divergence-measure field $(\rho, f(\rho))$ defined in [7], and we have applied the Gauss-Green formula and the existence of strong traces guaranteed by [22]. Passing to the limit in the first and last integral we get

$$\begin{aligned}\int_0^\infty F(t)\varphi(t,0)\ dt &\geq \int_0^\infty \int_0^\infty \left(\rho\ \partial_t \varphi + f(\rho)\partial_x \varphi\right) dx\ dt \\ &= \int_0^\infty f(\rho(t,0+))\ \varphi(t,0)\ dt,\end{aligned}$$

where the last inequality results from the fact that ρ is a weak entropy solution of (1.1) on $\mathbb{R}^+ \times \mathbb{R}^+$, again by [7, 22], see also [1, Remark 2]. Since the above inequality holds for all $\varphi \in \mathbf{C_c^1}(\mathbb{R}^+ \times \mathbb{R}; \mathbb{R}^+)$, we conclude that ρ satisfy (2.7).

To conclude the proof of Theorem 2.7, we have to verify that (2.15) still holds in the case of non-concave fluxes.

We consider the entropy formulation (2.6) with test functions $\varphi \in \mathbf{C_c^1}(\mathbb{R}^+ \times \mathbb{R}\backslash\{x=0\}; \mathbb{R}^+)$. The method of doubling of variables of Kruzhkov, applied in the domains $\{\pm x > 0\}$, yields the so-called Kato inequality for the comparison of ρ^1, ρ^2:

$$\int_{\mathbb{R}^+} \int_{\mathbb{R}} \Big(|\rho^1 - \rho^2| \partial_t + \Phi(\rho^1, \rho^2)\partial_x \Big)\ \varphi\ dx\ dt \geq 0.$$

Now, fix $R > 0$ and replace φ in this inequality by a sequence of approximations of the characteristic function of the set $\{t \in (0,T), 0 < |x| < R + L(T-t)\}$, for instance $\varphi_\varepsilon(t,x) = (1 - w_\varepsilon(x))\chi_\varepsilon(t)\xi_\varepsilon(t,x)$ where

$$\chi_\varepsilon(t) = \begin{cases} 1 & \text{if } 0 \le t < T, \\ \dfrac{T-t}{\varepsilon} + 1 & \text{if } T \le t < T+\varepsilon, \\ 0 & \text{if } t \ge T+\varepsilon, \end{cases}$$

w_ε is given by (2.8), and

$$\xi_\varepsilon(t,x) = \begin{cases} 1 & \text{if } |x| \le R + L(T-t), \\ \dfrac{R + L(T-t) - |x|}{\varepsilon} + 1 & \text{if } R + L(T-t) \le |x| < R + L(T-t) + \varepsilon, \\ 0 & \text{if } |x| \ge R + L(T-t) + \varepsilon. \end{cases}$$

This provides at the limit $\varepsilon \to 0$

$$- \int_{-R}^{R} |\rho^1 - \rho^2|(T,x)\, dx + \int_{-R-LT}^{R+LT} |\rho_0^1 - \rho_0^2|(x)\, dx \\ + \int_0^T \Big(\Phi(\rho^1(t,0+), \rho^2(t,0+)) - \Phi(\rho^1(t,0-), \rho^2(t,0-)) \Big)\, dt \ge 0. \quad (6.5)$$

Fix $t > 0$; without loss of generality, we can assume that $F^1(t) \ge F^2(t)$. We make a case study quite similar to the one of the proof of Lemma 2.6.

- If $(\rho^i(t,0-), \rho^i(t,0+)) \in \mathcal{G}_2(F^i) \cup \mathcal{G}_3(F^i)$, $i = 1,2$, then both the standing waves

  $$\tilde\rho^i(t,x) := \rho^i(t,0-)\mathbb{1}_{\{x<0\}} + \rho^i(t,0+)\mathbb{1}_{\{x>0\}},$$

  $i = 1,2$, are Kruzhkov entropy solutions of the (unconstrained) conservation law (1.1). Therefore we have the inequality

  $$\Phi(\rho^1(t,0+), \rho^2(t,0+)) - \Phi(\rho^1(t,0-), \rho^2(t,0-)) \le 0 \quad (6.6)$$

  which is well known since the work of Vol′pert [24].

- If $(\rho^1(t,0-), \rho^1(t,0+)) \in \mathcal{G}_1(F^1)$ and $(\rho^2(t,0-), \rho^2(t,0+)) \in \mathcal{G}_2(F^2) \cup \mathcal{G}_3(F^2)$, then we can use (2.13) to justify (6.6). Indeed, the definition of $\mathcal{G}_j$ and assumption $F^1 \ge F^2$ lead to the inclusions $\mathcal{G}_j(F^2) \subset \mathcal{G}_j(F^1)$ for $j = 2,3$.

- If $(\rho^1(t,0-), \rho^1(t,0+)) \in \mathcal{G}_2(F^1)$ and $(\rho^2(t,0-), \rho^2(t,0+)) \in \mathcal{G}_1(F^2)$, then $\rho^1(t,0-) = \rho^1(t,0+) =: \rho^1(t,0)$, $f(\rho^1(t,0)) \le F^1$ and $\rho^2(t,0+) < \rho^2(t,0-)$. We have to distinguish three cases:

– if $\rho^1(t,0) \le \rho^2(t,0+)$,

$$\begin{aligned}&\Phi(\rho^1(t,0),\rho^2(t,0+)) - \Phi(\rho^1(t,0),\rho^2(t,0-))\\ &= f(\rho^2(t,0+)) - f(\rho^1(t,0)) - f(\rho^2(t,0-)) + f(\rho^1(t,0)) = 0\,;\end{aligned}$$

– if $\rho^2(t,0+) < \rho^1(t,0) < \rho^2(t,0-)$,

$$\begin{aligned}&\Phi(\rho^1(t,0),\rho^2(t,0+)) - \Phi(\rho^1(t,0),\rho^2(t,0-))\\ &= f(\rho^1(t,0)) - f(\rho^2(t,0+)) - f(\rho^2(t,0-)) + f(\rho^1(t,0)) \le 2(F^1 - F^2)\,;\end{aligned}$$

– if $\rho^1(t,0) \ge \rho^2(t,0-)$,

$$\begin{aligned}&\Phi(\rho^1(t,0),\rho^2(t,0+)) - \Phi(\rho^1(t,0),\rho^2(t,0-))\\ &= f(\rho^1(t,0)) - f(\rho^2(t,0+)) - f(\rho^1(t,0)) + f(\rho^2(t,0-)) = 0\,.\end{aligned}$$

- If $(\rho^1(t,0-),\rho^1(t,0+)) \in \mathcal{G}_3(F^1)$ and $(\rho^2(t,0-),\rho^2(t,0+)) \in \mathcal{G}_1(F^2)$, we have for sure $\rho^2(t,0+) < \rho^2(t,0-)$. We have to detail several possibilities:

  – if $\rho^1(t,0\pm) \le \rho^2(t,0+)$,

$$\begin{aligned}&\Phi(\rho^1(t,0+),\rho^2(t,0+)) - \Phi(\rho^1(t,0-),\rho^2(t,0-))\\ &= f(\rho^2(t,0+)) - f(\rho^1(t,0+)) - f(\rho^2(t,0-)) + f(\rho^1(t,0-)) = 0\,;\end{aligned}$$

  – if $\rho^1(t,0\pm) \ge \rho^2(t,0-)$,

$$\begin{aligned}&\Phi(\rho^1(t,0+),\rho^2(t,0+)) - \Phi(\rho^1(t,0-),\rho^2(t,0-))\\ &= f(\rho^1(t,0+)) - f(\rho^2(t,0+)) - f(\rho^1(t,0-)) + f(\rho^2(t,0-)) = 0\,;\end{aligned}$$

  – if $\rho^2(t,0+) \le \rho^1(t,0\pm) \le \rho^2(t,0-)$,

$$\begin{aligned}&\Phi(\rho^1(t,0+),\rho^2(t,0+)) - \Phi(\rho^1(t,0-),\rho^2(t,0-))\\ &= f(\rho^1(t,0+)) - f(\rho^2(t,0+)) - f(\rho^2(t,0-)) + f(\rho^1(t,0-)) \le 2(F^1 - F^2)\,;\end{aligned}$$

  – if $\rho^2(t,0+) \le \rho^1(t,0-) \le \rho^2(t,0-) \le \rho^1(t,0+)$,

$$\begin{aligned}&\Phi(\rho^1(t,0+),\rho^2(t,0+)) - \Phi(\rho^1(t,0-),\rho^2(t,0-))\\ &= f(\rho^1(t,0+)) - f(\rho^2(t,0+)) - f(\rho^2(t,0-)) + f(\rho^1(t,0-)) \le 2(F^1 - F^2)\,;\end{aligned}$$

  – if $\rho^1(t,0-) \le \rho^2(t,0+) \le \rho^1(t,0+) \le \rho^2(t,0-)$,

$$\begin{aligned}&\Phi(\rho^1(t,0+),\rho^2(t,0+)) - \Phi(\rho^1(t,0-),\rho^2(t,0-))\\ &= f(\rho^1(t,0+)) - f(\rho^2(t,0+)) - f(\rho^2(t,0-)) + f(\rho^1(t,0-)) \le 2(F^1 - F^2)\,.\end{aligned}$$

- If $(\rho^i(t,0-),\rho^i(t,0+)) \in \mathcal{G}_1(F^i)$, $i=1,2$, then $f(\rho^i(t,0\pm)) = F^i$ and

$$\begin{aligned}&\Phi(\rho^1(t,0+),\rho^2(t,0+)) - \Phi(\rho^1(t,0-),\rho^2(t,0-))\\ &\leq \Big|f(\rho^1(t,0+)) - f(\rho^2(t,0+))\Big| + \Big|f(\rho^1(t,0-)) - f(\rho^2(t,0-))\Big| = 2(F^1 - F^2).\end{aligned}$$

Thus in all cases, we have

$$\Phi(\rho^1(t,0+),\rho^2(t,0+)) - \Phi(\rho^1(t,0-),\rho^2(t,0-)) \leq 2|F^1 - F^2|(t).$$

Hence

$$\int_{-R}^{R} |u^1 - u^2|(T,x)\, dx \leq \int_0^T 2|F^1 - F^2|(t)\, dt + \int_{-R-LT}^{R+LT} |u_0^1 - u_0^2|(x)\, dx;$$

letting R tend to $+\infty$, we conclude the proof.

Appendix

Lemma 6.1 *For any $n \in \mathbb{N}$ and $(\rho_o^n, F^n) \in \bar{\mathcal{D}}_n$, let ρ^n be the approximate solution to* (1.1)-(1.3) *obtained by wave-front tracking. At any waves interaction, the map $t \mapsto \Upsilon(t) = \Upsilon\left(\rho^n(t), F^n(\cdot + t)\right)$*

either *decreases by at least 2^{-n},*

or *remains constant and the number of waves does not increase.*

Proof. The proof is obtained considering the different interactions separately, depending on the position of the interaction point $\bar{x}$ and on the flows of the interacting states. We will consider interaction points $\bar{x} \leq 0$, the case $\bar{x} \geq 0$ being symmetric. It is not restrictive to assume that at any interaction time either two waves interact or a single wave hits $x = 0$.

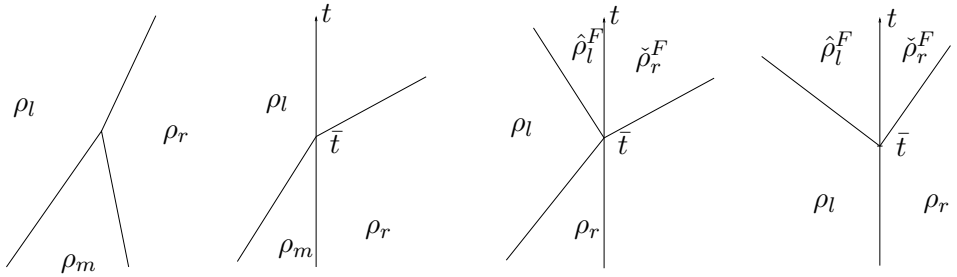

Figure 9: Notations for the proof of Lemma 6.1.

(I1) $\bar{x} \neq 0$. As in the usual scalar case, either two shocks collide (and the number of waves diminishes) or a shock and a rarefaction cancel (and $\mathrm{TV}(\Psi(\rho))$ diminishes), see Figure 9, left.

(I2) A wave hits $\bar{x} = 0$ at time $t = \bar{t}$ coming from the left. We have to distinguish between several situations.
Assume first that $\rho_m = \rho_r$. If $\mathcal{R}^F(\rho_l, \rho_r) = \mathcal{R}(\rho_l, \rho_r)$, then the wave simply crosses $x = 0$ and $\Delta\Upsilon(\bar{t}) = \Upsilon(\bar{t}+) - \Upsilon(\bar{t}-) = 0$. Otherwise, $f(\rho_l) > F$ and $\hat{\rho}_l^F > \rho_l$. This implies

$$\begin{aligned}\Delta\Upsilon(\bar{t}) &= \left|\Psi(\rho_l) - \Psi(\hat{\rho}_l^F)\right| + \left|\Psi(\hat{\rho}_l^F) - \Psi(\check{\rho}_r^F)\right| \\ &\quad + \left|\Psi(\check{\rho}_l^F) - \Psi(\rho_r)\right| + \gamma - \left|\Psi(\rho_l) - \Psi(\rho_r)\right| - \gamma_o \\ &= 2\Psi(\hat{\rho}_l^F) - 2\Psi(\rho_l) + \gamma - \gamma_o \leq -2^{1-n}.\end{aligned}$$

Above, $\gamma = 0, \gamma_a, \gamma_b, \gamma_c$ depending on the situation.

Let us consider now the case in which the wave (ρ_m, ρ_r) is an entropic shock. If $\mathcal{R}^F(\rho_l, \rho_r) = \mathcal{R}(\rho_l, \rho_r)$, then either two shocks collide (and the number of waves diminishes) or a shock and a rarefaction cancel (and $\mathrm{TV}(\Psi(\rho))$ diminishes), and $\gamma = \gamma_o$ remains constant.
If $\mathcal{R}^F(\rho_l, \rho_r) \neq \mathcal{R}(\rho_l, \rho_r)$, we have $\rho_l > \rho_r$ and $f(\rho_m) = f(\rho_r) \leq F$, hence $\check{\rho}_r^F \geq \rho_r$. We can estimate

$$\begin{aligned}\Delta\Upsilon(\bar{t}) &\leq \left|\Psi(\rho_l) - \Psi(\hat{\rho}_l^F)\right| + \left|\Psi(\hat{\rho}_l^F) - \Psi(\check{\rho}_r^F)\right| \\ &\quad + \left|\Psi(\check{\rho}_r^F) - \Psi(\rho_r)\right| + \gamma - \left|\Psi(\rho_l) - \Psi(\rho_r)\right| - \gamma_o.\end{aligned}$$

If $\rho_l \geq \hat{\rho}_l^F$, we have $\Delta\Upsilon(\bar{t}) \leq \gamma - \gamma_0 \leq -2^{2-n}$. If $\rho_l < \hat{\rho}_l^F$ (and hence $f(\rho_l) > F$), we obtain

$$\Delta\Upsilon(\bar{t}) \leq 2\Psi(\hat{\rho}_l^F) - 2\Psi(\rho_l) + \gamma - \gamma_o \leq -2^{1-n}.$$

Assume now that the wave $(\rho_m, \rho_r) \in \mathcal{G}_1$ is a nonclassical shock resulting from the application of $\mathcal{R}^F$. If the segment joining $f(\rho_m)$ and $f(\rho_r)$ does not intersect the graph of f, then $\rho_l < \rho_r$, no new wave is created and easy calculations show that

$$\begin{aligned}\Delta\Upsilon(\bar{t}) &= \left|\Psi(\rho_l) - \Psi(\rho_r)\right| + \gamma_o \\ &\quad - \left|\Psi(\rho_l) - \Psi(\rho_m)\right| - \left|\Psi(\rho_m) - \Psi(\rho_r)\right| \\ &= 2\Psi(\rho_r) - 2\Psi(\rho_m) + \gamma_o = 0.\end{aligned}$$

If $(\rho_m, \rho_r) \in \mathcal{G}_1^a$ and $F^n(\bar{t}) > f(r)$, then $\rho_l \geq r$ and we have

$$\begin{aligned}\Delta\Upsilon(\bar{t}) &= \left|\Psi(\rho_l) - \Psi(\hat{\rho}_l^F)\right| + \left|\Psi(\hat{\rho}_l^F) - \Psi(\rho_r)\right| + \gamma_c \\ &\quad - \left|\Psi(\rho_l) - \Psi(\rho_m)\right| - \left|\Psi(\rho_m) - \Psi(\rho_r)\right| - \gamma_a \\ &= 2\Psi(\rho_l) - 2\Psi(\rho_m) + \gamma_c - \gamma_a \\ &= 2(f(\rho_l) - F^n(\bar{t})) \leq -2^{1-n}.\end{aligned}$$

The case $(\rho_m, \rho_r) \in \mathcal{G}_1^b$ is similar. Finally, if $(\rho_m, \rho_r) \in \mathcal{G}_1^c$, we have to distinguish two cases, depending on the position of ρ_l. If $\rho_l < \rho_r$, the case can be treated as above. If $r < \rho_l < R_M^*$, then $\hat{\rho}_l^F > \rho_l$ and $(\hat{\rho}_l^F, \rho_r) \in \mathcal{G}_1^a$. Then the number of waves remains constant and

$$\begin{aligned}\Delta\Upsilon(\bar{t}) &= \left|\Psi(\rho_l) - \Psi(\hat{\rho}_l^F)\right| + \left|\Psi(\hat{\rho}_l^F) - \Psi(\rho_r)\right| + \gamma_a \\ &\quad - \left|\Psi(\rho_l) - \Psi(\rho_m)\right| - \left|\Psi(\rho_m) - \Psi(\rho_r)\right| - \gamma_c \\ &= 2\Psi(\hat{\rho}_l^F) - 2\Psi(\rho_l) + \gamma_a - \gamma_c \leq 0.\end{aligned}$$

(I3) A wave hits $\bar{x} = 0$ at time $t = \bar{t}$ coming from the right. If $\rho_l = \rho_m$ and $\mathcal{R}^F(\rho_l, \rho_r) \neq \mathcal{R}(\rho_l, \rho_r)$, then it must be $f(\rho_r) > F$ and $\check{\rho}_r^F < \rho_r$ (and $f(\rho_l) \leq F$ and $\hat{\rho}_l^F \leq \rho_l$). We have

$$\begin{aligned}\Delta\Upsilon(\bar{t}) &= \left|\Psi(\rho_l) - \Psi(\hat{\rho}_l^F)\right| + \left|\Psi(\hat{\rho}_l^F) - \Psi(\check{\rho}_r^F)\right| \\ &\quad + \left|\Psi(\check{\rho}_l^F) - \Psi(\rho_r)\right| + \gamma - \left|\Psi(\rho_l) - \Psi(\rho_r)\right| - \gamma_o \\ &= 2\Psi(\rho_r) - 2\Psi(\check{\rho}_r^F) + \gamma - \gamma_o \\ &\leq 2\left(F - f(\rho_r)\right) \leq -2^{1-n}.\end{aligned}$$

Above, $\gamma = 0, \gamma_a, \gamma_b, \gamma_c$ depending on the situation.

Let us now assume that (ρ_l, ρ_m) is an entropic shock, and $\mathcal{R}^F(\rho_l, \rho_r) \neq \mathcal{R}(\rho_l, \rho_r)$. Then we have $f(\rho_l) = f(\rho_m) \leq F$, and thus $\hat{\rho}_l^F \leq \rho_l$. Moreover, $\rho_r < \rho_l$. Then

$$\begin{aligned}\Delta\Upsilon(\bar{t}) &\leq \left|\Psi(\rho_l) - \Psi(\hat{\rho}_l^F)\right| + \left|\Psi(\hat{\rho}_l^F) - \Psi(\check{\rho}_r^F)\right| \\ &\quad + \left|\Psi(\check{\rho}_r^F) - \Psi(\rho_r)\right| + \gamma - \left|\Psi(\rho_l) - \Psi(\rho_r)\right| - \gamma_o \\ &= \Psi(\rho_r) - \Psi(\check{\rho}_r^F) + \left|\Psi(\check{\rho}_r^F) - \Psi(\rho_r)\right| + \gamma - \gamma_o.\end{aligned}$$

If $\rho_r \leq \check{\rho}_r^F$, we have $\Delta\Upsilon(\bar{t}) \leq \gamma - \gamma_0 \leq -2^{2-n}$. If $\rho_l > \hat{\rho}_l^F$ (and hence $f(\rho_r) > F$), we obtain

$$\Delta\Upsilon(\bar{t}) \leq 2\Psi(\rho_r) - 2\Psi(\check{\rho}_r^F) + \gamma - \gamma_o \leq 2\left(F - f(\rho_r)\right) \leq -2^{1-n}.$$

Assume now that the wave $(\rho_l, \rho_m) \in \mathcal{G}_1$ is a nonclassical shock resulting from the application of $\mathcal{R}^F$. If the segment joining $f(\rho_l)$ and $f(\rho_m)$ does not intersect the graph of f, then $\rho_l < \rho_r$, no new wave is created and easy calculations show that

$$\begin{aligned}\Delta\Upsilon(\bar{t}) &= \left|\Psi(\rho_l) - \Psi(\rho_r)\right| + \gamma_o \\ &\quad - \left|\Psi(\rho_l) - \Psi(\rho_m)\right| - \left|\Psi(\rho_m) - \Psi(\rho_r)\right| \\ &= 2\Psi(\rho_m) - 2\Psi(\rho_l) + \gamma_o = 0.\end{aligned}$$

If $(\rho_l, \rho_m) \in \mathcal{G}_1^a$ and $F^n(\bar{t}) > f(r)$, then the case $\rho_l < \rho_r$ can be treated as the previous case. Otherwise, if $R_M < \rho_r \leq r$, we have

$$\begin{aligned}\Delta\Upsilon(\bar{t}) &= \left|\Psi(\rho_l) - \Psi(\check{\rho}_r^F)\right| + \left|\Psi(\check{\rho}_r^F) - \Psi(\rho_r)\right| + \gamma_b \\ &\quad - \left|\Psi(\rho_l) - \Psi(\rho_m)\right| - \left|\Psi(\rho_m) - \Psi(\rho_r)\right| - \gamma_a \\ &= 2\Psi(\rho_m) - 2\Psi(\rho_r) + \gamma_b - \gamma_a \\ &= 2(f(\rho_r) - F^n) \leq -2^{1-n}.\end{aligned}$$

The case $(\rho_l, \rho_m) \in \mathcal{G}_1^c$ is similar. Finally, if $(\rho_l, \rho_m) \in \mathcal{G}_1^b$, we have to distinguish two cases, depending on the position of ρ_r. If $\rho_r > \rho_m$, the case can be treated as above. If $\rho_r < \rho_m \leq r$, then $f(\rho_r) > F$ and $\check{\rho}_r^F < \rho_r$ and $(\rho_l, \check{\rho}_r^F) \in \mathcal{G}_1^a$. Then the number of waves remains constant and

$$\begin{aligned}\Delta\Upsilon(\bar{t}) &= \left|\Psi(\rho_l) - \Psi(\check{\rho}_r^F)\right| + \left|\Psi(\check{\rho}_r^F) - \Psi(\rho_r)\right| + \gamma_a \\ &\quad - \left|\Psi(\rho_l) - \Psi(\rho_m)\right| - \left|\Psi(\rho_m) - \Psi(\rho_r)\right| - \gamma_b \\ &= 2\Psi(\rho_r) - 2\Psi(\check{\rho}_r^F) + \gamma_a - \gamma_b \\ &= 2\left(F - f(\rho_r)\right) \leq 0.\end{aligned}$$

(I4) The constraint F^n jumps downward, see Fig. 9, right. We have to check several cases.
If $\rho_l = \rho_r = \rho$ and $F^n(\bar{t}+) < f(\rho) \leq F^n(\bar{t}-)$, two waves will exit the point $(\bar{t}, 0)$ with $\check{\rho}^F < \rho < \hat{\rho}^F$:

$$\begin{aligned}\Delta\Upsilon(\bar{t}) &= \left|\Psi(\rho) - \Psi(\hat{\rho}^F)\right| + \left|\Psi(\hat{\rho}^F) - \Psi(\check{\rho}^F)\right| \\ &\quad + \left|\Psi(\check{\rho}^F) - \Psi(\rho)\right| + \gamma - \gamma_o - 5\left|F^n(\bar{t}+) - F^n(\bar{t}-)\right| \\ &= 2\Psi(\hat{\rho}^F) - 2\Psi(\check{\rho}^F) + \gamma - \gamma_o - 5\left|F^n(\bar{t}+) - F^n(\bar{t}-)\right| \\ &= -5\left|F^n(\bar{t}+) - F^n(\bar{t}-)\right| \leq -5 \times 2^{-n}.\end{aligned}$$

Above, $\gamma = 0, \gamma_b$ or γ_c, depending on the position of ρ.
If (ρ_l, ρ_r) is an entropic shock, and $F^n(\bar{t}+) < f(\rho_l) = f(\rho_r) \leq F^n(\bar{t}-)$, then

$$\begin{aligned}\Delta\Upsilon(\bar{t}) &= \left|\Psi(\rho_l) - \Psi(\hat{\rho}_l^F)\right| + \left|\Psi(\hat{\rho}_l^F) - \Psi(\check{\rho}_r^F)\right| + \left|\Psi(\check{\rho}_r^F) - \Psi(\rho_r)\right| \\ &\quad + \gamma - \left|\Psi(\rho_l) - \Psi(\rho_r)\right| - \gamma_o - 5\left|F^n(\bar{t}+) - F^n(\bar{t}-)\right|.\end{aligned}$$

Therefore, if $\rho_r < r < \rho_l$, then $\check{\rho}_r^F < \rho_r < \rho_l < \hat{\rho}_l^F$ and $(\hat{\rho}_l^F, \check{\rho}_r^F) \in \mathcal{G}_1^a$:

$$\begin{aligned}\Delta\Upsilon(\bar{t}) &\leq 2\Psi(\hat{\rho}_l^F) - 2\Psi(\check{\rho}_r^F) + 2\Psi(\rho_r) - 2\Psi(\rho_l) \\ &\quad + \gamma_a - \gamma_o - 5\left(F^n(\bar{t}-) - F^n(\bar{t}+)\right) \\ &= -4\left(f(\rho_l) - f(r)\right) + 4\left(F^n(\bar{t}+) - f(r)\right) - \left(F^n(\bar{t}-) - F^n(\bar{t}+)\right) \\ &\leq -2^{-n};\end{aligned}$$

otherwise, if $\rho_l < \rho_r$, then $\check{\rho}_r^F < \rho_l < \rho_r < \hat{\rho}_l^F$:

$$\begin{aligned}\Delta\Upsilon(\bar{t}) &\leq 2\Psi(\hat{\rho}_l^F) - 2\Psi(\check{\rho}_r^F) + \gamma - \gamma_o - 5\left(F^n(\bar{t}-) - F^n(\bar{t}+)\right)\\ &= -\left(F^n(\bar{t}-) - F^n(\bar{t}+)\right) \leq -2^{-n}.\end{aligned}$$

Finally, if (ρ_l, ρ_r) is a nonclassical shock, and $F^n(\bar{t}+) < f(\rho_l) = f(\rho_r) = F^n(\bar{t}-)$, then $\check{\rho}_r^F < \rho_r < \rho_l < \hat{\rho}_l^F$ and

$$\begin{aligned}\Delta\Upsilon(\bar{t}) &\leq 2\Psi(\hat{\rho}_l^F) - 2\Psi(\check{\rho}_r^F) + 2\Psi(\rho_r) - 2\Psi(\rho_l)\\ &\quad + \gamma(\bar{t}+) - \gamma(\bar{t}-) - 5\left(F^n(\bar{t}-) - F^n(\bar{t}+)\right)\\ &\leq -\left(F^n(\bar{t}-) - F^n(\bar{t}+)\right) \leq -2^{-n}.\end{aligned}$$

(I5) The constraint F^n jumps upward. We need to check only the case in which (ρ_l, ρ_r) is a nonclassical shock, and $F^n(\bar{t}+) > f(\rho_l) = f(\rho_r) = F^n(\bar{t}-)$.
If $f\left(\mathcal{R}(\rho_l, \rho_r)(0)\right) \leq F^n(\bar{t}+)$, then the solution become classical and the variation of the functional can be estimated as follows

$$\begin{aligned}\Delta\Upsilon(\bar{t}) &= \left|\Psi(\rho_l) - \Psi(\rho_r)\right| + \gamma_o(\bar{t}+)\\ &\quad - \left|\Psi(\rho_l) - \Psi(\rho_r)\right| - \gamma(\bar{t}-) - 5\left(F^n(\bar{t}-) - F^n(\bar{t}+)\right)\\ &\leq -\left(F^n(\bar{t}-) - F^n(\bar{t}+)\right) \leq -2^{-n}.\end{aligned}$$

Otherwise, if $f\left(\mathcal{R}(\rho_l, \rho_r)(0)\right) > F^n(\bar{t}+)$, we still have a nonclassical shock and $\rho_r < \check{\rho}_r^F < \hat{\rho}_l^F < \rho_l$:

$$\begin{aligned}\Delta\Upsilon(\bar{t}) &= \left|\Psi(\hat{\rho}_l^F) - \Psi(\check{\rho}_r^F)\right| + \gamma(\bar{t}+)\\ &\quad - \left|\Psi(\rho_l) - \Psi(\rho_r)\right| - \gamma(\bar{t}-) - 5\left(F^n(\bar{t}-) - F^n(\bar{t}+)\right)\\ &\leq -\left(F^n(\bar{t}-) - F^n(\bar{t}+)\right) \leq -2^{-n}.\end{aligned}$$

Indeed, observe that

$$\left|\Psi(\hat{\rho}_l^F) - \Psi(\check{\rho}_r^F)\right| \leq \left|\Psi(\rho_l) - \Psi(\rho_r)\right|$$

and

$$\gamma(\bar{t}+) - \gamma(\bar{t}-) - 5\left(F^n(\bar{t}-) - F^n(\bar{t}+)\right) \leq -\left(F^n(\bar{t}-) - F^n(\bar{t}+)\right).$$

□

Acknowlegments

The second author was partially supported by the ERC Starting Grant 2010 under the project *"TRAffic Management by Macroscopic Models"*.

References

[1] B. Andreianov, P. Goatin, and N. Seguin. Finite volume schemes for locally constrained conservation laws. *Numer. Math.*, 115(4):609–645, 2010. With supplementary material available online.

[2] D. Braess. Über ein Paradoxon aus der Verkehrsplanung. *Unternehmensforschung*, 12:258–268, 1968.

[3] A. Bressan. *Hyperbolic systems of conservation laws*, volume 20 of *Oxford Lecture Series in Mathematics and its Applications*. Oxford University Press, Oxford, 2000. The one-dimensional Cauchy problem.

[4] R. Bürger, A. García, K. H. Karlsen, and J. D. Towers. A family of numerical schemes for kinematic flows with discontinuous flux. *J. Engrg. Math.*, 60(3-4):387–425, 2008.

[5] C. Chalons. Numerical approximation of a macroscopic model of pedestrian flows. *SIAM J. Sci. Comput.*, 29(2):539–555 (electronic), 2007.

[6] C. Chalons and P. Goatin. Transport-equilibrium schemes for computing contact discontinuities in traffic flow modeling. *Commun. Math. Sci.*, 5(3):533–551, 2007.

[7] G.-Q. Chen and H. Frid. Divergence-measure fields and hyperbolic conservation laws. *Arch. Ration. Mech. Anal.*, 147(2):89–118, 1999.

[8] P. Colella. Glimm's method for gas dynamics. *SIAM J. Sci. Statist. Comput.*, 3(1):76–110, 1982.

[9] R. M. Colombo and P. Goatin. A well posed conservation law with a variable unilateral constraint. *J. Differential Equations*, 234(2):654–675, 2007.

[10] R. M. Colombo, P. Goatin, and M. D. Rosini. Conservation laws with unilateral constraints in traffic modeling. In *Applied and industrial mathematics in Italy III*, volume 82 of *Ser. Adv. Math. Appl. Sci.*, pages 244–255. World Sci. Publ., Hackensack, NJ, 2010.

[11] R. M. Colombo, P. Goatin, and M. D. Rosini. On the modelling and management of traffic. *ESAIM Math. Model. Numer. Anal.*, 45(5):853–872, 2011.

[12] R. M. Colombo and M. D. Rosini. Pedestrian flows and non-classical shocks. *Math. Methods Appl. Sci.*, 28(13):1553–1567, 2005.

[13] R. M. Colombo and M. D. Rosini. Existence of nonclassical solutions in a pedestrian flow model. *Nonl. Analysis: RWA*, 10:2716–2728, 2009.

[14] M. Crandall and L. Tartar. Some relations between nonexpansive and order preserving mappings. *Proc. AMS*, 78(3):385–390, 1980.

[15] C. M. Dafermos. Polygonal approximations of solutions of the initial value problem for a conservation law. *J. Math. Anal. Appl.*, 38:33–41, 1972.

[16] M. L. Delle Monache and P. Goatin. Scalar conservation laws with moving density constraints arising in traffic flow modeling. in preparation.

[17] M. Garavello and P. Goatin. The Aw-Rascle traffic model with locally constrained flow. *J. Math. Anal. Appl.*, 378(2):634–648, 2011.

[18] M. Garavello and B. Piccoli. *Traffic flow on networks*, volume 1 of *AIMS Series on Applied Mathematics*. American Institute of Mathematical Sciences (AIMS), Springfield, MO, 2006. Conservation laws models.

[19] D. Helbing, A. Johansson, and H. Z. Al-Abideen. Dynamics of crowd disasters: An empirical study. *Physical Review E*, 75(2), 2007.

[20] P. G. Lefloch. *Hyperbolic systems of conservation laws*. Lectures in Mathematics ETH Zürich. Birkhäuser Verlag, Basel, 2002. The theory of classical and nonclassical shock waves.

[21] T. P. Liu. The Riemann problem for general systems of conservation laws. *J. Differential Equations*, 18:218–234, 1975.

[22] E. Y. Panov. Existence of strong traces for quasi-solutions of multidimensional conservation laws. *J. Hyperbolic Differ. Equ.*, 4(4):729–770, 2007.

[23] B. Temple. Global solution of the Cauchy problem for a class of 2×2 nonstrictly hyperbolic conservation laws. *Adv. in Appl. Math.*, 3(3):335–375, 1982.

[24] A. I. Vol′pert. Spaces BV and quasilinear equations. *Mat. Sb. (N.S.)*, 73 (115):255–302, 1967.